Trajectory Optimization of Chance-Constrained Nonlinear Stochastic Systems for Motion Planning and Control

Yashwanth Kumar Nakka, *Student Member, IEEE*, and Soon-Jo Chung, *Member, IEEE*

arXiv:2106.02801v1 [cs.RO] 5 Jun 2021

Abstract—We present gPC-SCP: *G*eneralized *P*olynomial *Ch*aos-based *S*equential *C*onvex *P*rogramming method to compute a sub-optimal solution for a continuous-time chance-constrained stochastic nonlinear optimal control problem (SNOC) problem. The approach enables motion planning and control of robotic systems under uncertainty. The proposed method involves two steps. The first step is to derive a deterministic nonlinear optimal control problem (DNOC) with convex constraints that are surrogate to the SNOC by using gPC expansion and the distributionally-robust convex subset of the chance constraints. The second step is to solve the DNOC problem using sequential convex programming (SCP) for trajectory generation and control. We prove that in the unconstrained case, the optimal value of the DNOC converges to that of SNOC asymptotically and that any feasible solution of the constrained DNOC is a feasible solution of the chance-constrained SNOC. We derive a stable stochastic model predictive controller using the gPC-SCP for tracking a trajectory in the presence of uncertainty. We empirically demonstrate the efficacy of the gPC-SCP method for the following three test cases: 1) collision checking under uncertainty in actuation, 2) collision checking with stochastic obstacle model, and 3) safe trajectory tracking under uncertainty in the dynamics and obstacle location by using a receding horizon control approach. We validate the effectiveness of the gPC-SCP method on the robotic spacecraft testbed.

I. INTRODUCTION

CONFIDENCE-based motion planning [1]–[4] and control algorithms [5], [6], that incorporate uncertainties in the dynamic model and environment to guarantee safety and performance with high probability, enable safe operation of robots and autonomous systems in partially known and dynamic environments. A probabilistic approach can allow for integration with a higher-level discrete decision-making algorithm for information gathering [7], [8], and for safe exploration [9], [10] to learn the interaction with an unknown environment. Examples of autonomous systems that require safety guarantees under uncertainty include spacecraft with thrusters as actuators during proximity operations [8], [11], powered descent on Mars [12], and quadrotors flying in turbulent winds [13], [14].

Motion planning problem considering safety in conjunction with optimality under uncertainty can be formulated as a continuous-time continuous-space stochastic nonlinear optimal control problem (SNOC) with chance constraints. In this paper, we propose the generalized polynomial chaos-based sequential convex programming (gPC-SCP) method, as described
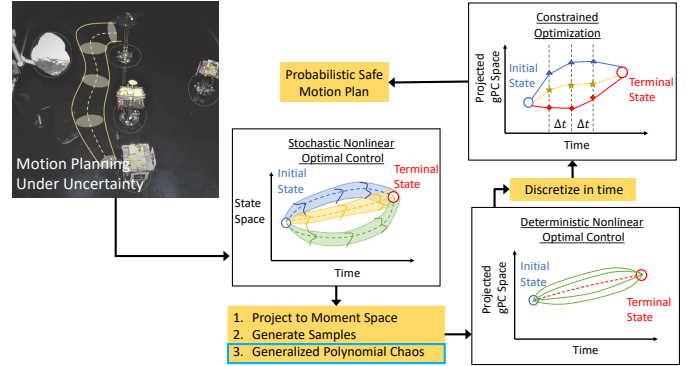
Fig. 1. Caltech's M-STAR [11] (Multi-Spacecraft Testbed for Autonomy Research) planning a safe trajectory to ensure safety under uncertainty in actuation during a proximity maneuver. The motion planning problem is formulated as a chance-constrained stochastic optimal control problem solved in two steps. Step 1: Project the stochastic problem to a deterministic problem by using generalized polynomial chaos approach and distributional robustness; and Step 2: Use deterministic solvers to compute an optimal solution to the deterministic problem.

in Fig. 1, to solve a chance-constrained SNOC problem. The method involves deriving a deterministic nonlinear optimal control (DNOC) problem with convex constraints that are a surrogate to the SNOC problem with linear and quadratic chance constraints. We derive the DNOC problem by accounting for nonlinear stochastic dynamics using generalized polynomial chaos expansions (gPC) [15]–[17] and obtaining deterministic convex approximations of linear and quadratic chance constraints using distributional robustness [18]–[20]. The DNOC problem is then solved using sequential convex programming (SCP) [21]–[23] for trajectory optimization and for nonlinear stochastic model predictive control (SMPC).

The main contributions of the paper are as follows:

(a) We present a systematic sequence of approximations for the chance-constrained SNOC problem to compute a convex-constrained DNOC problem using gPC projection. We analyze the gPC projection of the stochastic dynamics for existence and uniqueness [24], [25] of a solution in the gPC space. Examples are provided to study the effect of projection on both the controllability of surrogate dynamics and the feasibility of the DNOC problem. We prove the convexity of the distributionally-robust linear and quadratic chance constraints in the gPC space.

(b) In order to characterize the deterministic approximation obtained using gPC projection, we present analysis on convergence of the DNOC problem to the SNOC problem for the unconstrained case. Then, we prove that any

feasible solution of the constrained DNOC problem is a feasible solution of chance-constrained SNOC problem with an appropriate gPC transformation step applied.

(c) We derive provably conservative convex surrogates for collision checking with both deterministic and stochastic obstacle state models. We integrate this collision constraint with a sampling-based planning method [26], [27] to derive an algorithm that computes safe and optimal motion plans under uncertainty.

(d) We extend the gPC-SCP method to derive an iterative algorithm that solves the SMPC formulation. We prove that, if the terminal cost used in the SMPC problem is derived by an exponentially-stabilizing controller (e.g. [5]) for the stochastic dynamics, then the stochastic model predictive controller is stable and the cost converges to an upper bound.

(e) We validate the convergence and stability theorems, and the safety provided by the convex constraints in simulation, on a three degree-of-freedom robot dynamics. We show empirically that the gPC-SCP method, for both planning and control, has a higher success rate in comparison to the Gaussian approximation [6], [28] of the collision chance constraints. We demonstrate the efficacy of the gPC-SCP method by computing a safe trajectory for a spacecraft proximity maneuver under uncertainty in environment (obstacles) on the robotic spacecraft dynamics simulator [11] hardware platform and by executing the trajectory in real-time closed-loop experiments.

A. Related Work

Existing methods to solve a chance-constrained stochastic optimal control problem use moment space propagation [6], [29]–[31], unscented transformation-based propagation [32], Monte Carlo sample propagation [2], [3], [33], and scenario-based [32], [34] approaches to construct a deterministic surrogate problem. Although these methods alleviate the curse of dimensionality, they do not provide asymptotic convergence guarantees for a DNOC problem. Monte Carlo methods provide asymptotic convergence guarantees, but often require large samples to estimate the constraint satisfaction for nonlinear systems and use mixed-integer programming [2] solvers for computing a solution. We use gPC propagation [17] to construct a DNOC problem that converges to the SNOC problem, asymptotically. The gPC projection transforms the chance constraints from being a non-convex constraint in moment space to a convex constraint in the gPC space. This enables the use of sequential convex programming [21], [23] method for computing a solution. Additionally, we study the existence and uniqueness [35] of a solution and the controllability of the deterministic surrogate dynamics of the stochastic dynamics.

Earlier work [3], [6], [36] uses a Gaussian approximation of the linear and the quadratic chance constraint for collision checking and for terminal constraint satisfaction. While this avoids multi-dimensional integration of chance constraints for feasibility checking, Gaussian approximation might not be an equivalent representation (or) even a subset of the feasible set

in the presence of stochastic process noise in dynamics. We use distributional robustness [19], [20] property to propose a new deterministic second-order cone constraint and a quadratic constraint approximation of the linear and quadratic chance constraints. We prove that the deterministic approximations are a subset of the respective chance constraints.

In [2], [3], linear chance constraints were considered for probabilistic optimal planning for linear systems. The literature on chance-constrained programming focuses on problems with deterministic decision variable and uncertain system parameters for both linear [19] and nonlinear [20] cases. The results [18], [19] on distributional robust subset and convex approximations of the chance constraints can be readily transformed to the case with a random decision variable for an unknown measure. The quadratic chance constraint would lead to an inner semi-definite program [37] that adds complexity to the SNOC problem considered in this paper. The linear chance constraint for collision checking was first presented in [1]. In [38], authors show that linearized chance constraint is a subset of the original nonlinear chance constraint for a Gaussian confidence-based constraint. Since the local Gaussian assumption might not be valid for a nonlinear systems, we present proof for the distributionally robust convex constraint formulation that extends to include uncertainty in obstacle state for a nonlinear stochastic differential equation.

From a SMPC perspective, recent work [39]–[42] on control of discrete-time linear stochastic dynamical systems provides conditions for recursive feasibility, constraint satisfaction, convergence and stability by using a probabilistic invariant set as the domain of operation and a control Lyapunov function as the terminal cost function. Research on control of nonlinear stochastic dynamics [6], [43], [44] is focused on implementation by using nonlinear programming methods. In [45], authors formulate a bounding semi-definite optimization problem on moments using global polynomial optimization method [46] for controlling a nonlinear stochastic system, but do not incorporate state constraints or prove the stability of the system. We propose a SMPC method to control nonlinear stochastic differential equation that uses a stochastic control contraction metric [5], [47] as the terminal cost function. Assuming recursive feasibility and constraint satisfaction, we prove the convergence and stability of the SMPC method. We solve the SMPC problem using the gPC-SCP method to track a potentially unsafe trajectory in the presence of uncertainty in dynamics and environment.

The gPC expansion approach was used for stability analysis and control design of uncertain systems [43], [44], [48]–[51]. For trajectory optimization, recent work focused on nonlinear systems with parametric uncertainty [52], [53] with no constraints on the state, or linear systems with linear chance-constraints that do not extend to the SNOC problem considered here and lack analysis on the deterministic approximation of the uncertain system. The gPC approach was used to compute a moment-space receding horizon approximation [54], which was solved using nonlinear programming methods. We extend prior work to incorporate nonlinear dynamics and include analysis on the deterministic approximation. We formulate convex constraints for linear and quadratic constraints in gPC

space and use this formulation to design algorithms for motion planning and control of a nonlinear stochastic dynamic system.

We generalize and extend our prior conference paper [1] significantly as follows: i) we derive a sequence of approximations from a SNOC problem to the DNOC problem, which provides a modular architecture to understand trajectory optimization under uncertainty; ii) we include examples discussing the effect of gPC projection on the controllability of stochastic dynamics; iii) we design a motion planning algorithm to handle uncertainty in both dynamics and obstacle location, which takes advantage of the state-of-the-art sampling-based [26] planning algorithms; iv) we formulate a stochastic model predictive algorithm using the gPC-SCP method and provide conditions for its stability and convergence; and v) we validate the gPC-SCP approach empirically and on the spacecraft simulator hardware testbed.

Organization: We discuss the stochastic nonlinear optimal control (SNOC) problem with results on deterministic approximations of chance constraints along with preliminaries on gPC expansions in Section II. The deterministic surrogate of the SNOC problem in terms of the gPC coefficients and a SCP formulation of the DNOC problem are presented with analysis in Section III. In Sections IV and V, we apply the gPC-SCP method under uncertainty in dynamics and constraints for both motion planning using SNOC solutions and tracking control using model predictive control, respectively. In Section VI, we validate gPC-SCP method via simulations and experiments on robotic spacecraft dynamics simulator. We conclude the paper in Section VII with a brief discussion on the approach and impact of the method.

Notation: For a random variable $x \in \mathbb{R}^{d_x}$, μ_x is the mean, Σ_x is the covariance matrix, $\mathbb{R}$ is real line, d_x is the dimension of x. $\mathbb{E}$ and Pr are the expectation operation and probability measure, respectively. We define a deterministic vector as $\bar{x}$. The $p-$norm of a vector $\bar{u} \in \mathbb{R}^{d_u}$ is defined as $\|\bar{u}\|_p = (\sum_1^{d_u} |\bar{u}_i|^p)^{\frac{1}{p}}$. We use $\nabla_x = \frac{\partial}{\partial x}$, $\nabla_{xx} = \frac{\partial^2}{\partial x^2}$. The risk measure for constraint violation is ϵ. We define the gPC state using X and the indicator function as I. We use $\mathbb{I}$ for an identity matrix and $\mathbb{1}$ for a matrix with entries as 1. The Kronecker's product of two matrices $A_{m \times n}$ and $B_{p \times q}$ is defined as follows:

$$(A \otimes B)_{mp \times nq} = \begin{bmatrix} a_{11}B & \dots & a_{1n}B \\ \vdots & \ddots & \vdots \\ a_{m1}B & \dots & a_{mn}B \end{bmatrix},$$

where a_{ij} is the element at i^{th} row and j^{th} column of A. For a matrix A, $\mathrm{tr}(A)$ is the trace operation, $\lambda_{\min}(A)$ and $\lambda_{\max}(A)$ are the minimum and maximum eigenvalues of A.

II. PROBLEM AND PRELIMINARIES

In this section, we present the stochastic optimal control problem formulation, preliminaries on the relaxations used for chance constraints, and the generalized polynomial chaos approach that forms a basis for constructing a surrogate deterministic optimal control problem.

A. Stochastic Nonlinear Optimal Control Problem

We consider the finite-horizon stochastic nonlinear optimal control (SNOC) problem with joint chance constraints in continuous time and continuous space. The SNOC problem minimizes an expectation cost function, that is a sum of a quadratic function in the random state variable $x(t)$ and a convex norm of the control policy $\bar{u}(t)$. The evolution of the stochastic process $x(t)$ for all sampled paths is defined by a stochastic differential equation. The joint chance constraints guarantee constraint feasibility with a probability of $1 - \epsilon$, where $\epsilon > 0$ and is chosen to be a small value (example: $\epsilon \in [0.001, 0.05]$) for better constraint satisfaction. The following optimal control problem is considered with the state distribution and control as the decision variables.

Problem 1. *Chance-Constrained Stochastic Nonlinear Optimal Control.*

$$J_{\text{SNOC}}^* = \min_{x(t), \bar{u}(t)} \mathbb{E}\left[\int_{t_0}^{t_f} J(x(t), \bar{u}(t))dt + J_f(x(t_f)) \right] \quad (1)$$

$$s.t. \quad dx = f(x(t), \bar{u}(t))dt + g(x(t), \bar{u}(t))dw(t) \quad (2)$$

$$\mathrm{Pr}(x(t) \in \mathcal{X}_{\mathcal{F}}) \geq 1 - \epsilon \ \forall t \in [t_0, t_f] \quad (3)$$

$$\bar{u}(t) \in \mathcal{U} \quad \forall t \in [t_0, t_f] \quad (4)$$

$$x(t_0) = x_0 \quad x_{t_f} \in \mathcal{X}_f \quad (5)$$

The cost functional J and the terminal cost J_f are:

$$J(x(t), \bar{u}(t)) = x(t)^\top Q x(t) + \|\bar{u}\|_p, \text{ where } p \in \{1, 2, \infty\},$$
$$J_f(x(t_f)) = x(t_f)^\top Q_f x(t_f). \quad (6)$$

where Q and Q_f are positive definite matrices. The $p-$norm of a vector $\bar{u}$ is defined as $\|\bar{u}\|_p = (\sum_1^{d_u} |\bar{u}_i|^p)^{\frac{1}{p}}$. The terminal set $\mathcal{X}_f$ is the set of allowed realization of the state x after propagation. The terminal constraint is applied as a probabilistic soft constraint to ensure feasibility of Problem 1. In the following, we define each of the aforementioned elements of Problem 1 and discuss convex approximations of linear and quadratic chance constraints.

1) Stochastic Differential Equation (SDE) [35]: The dynamics of the system is modeled as a controlled diffusion process with Itô assumptions. The random variable $x(t)$ is defined on a probability space $(\Omega, \mathbb{F}, \mathrm{Pr})$ where Ω is the sample space, $\mathbb{F}$ forms a σ-field with measure Pr.

$$dx(t) = f(x(t), \bar{u}(t))dt + g(x(t), \bar{u}(t))dw(t),$$
$$\mathrm{Pr}(|x(t_0) - x_0| = 0) = 1, \quad \forall t_0 \leq t \leq t_f < \infty, \quad (7)$$

where: $f(.,.) : \mathcal{X} \times \mathcal{U} \to \mathbb{R}^{d_x}$, $g(.,.) : \mathcal{X} \times \mathcal{U} \to \mathbb{R}^{d_x \times d_\xi}$, and $w(t)$ is a d_ξ-dimensional Wiener process and the initial random variable x_0 is independent of $w(t) - w(t_0)$ for $t \geq t_0$, and $dw(t) \sim \mathcal{N}(0, dt\mathbb{I})$. The sets $\mathcal{X} \subseteq \mathbb{R}^{d_x}$ and $\mathcal{U} \subseteq \mathbb{R}^{d_u}$ are compact sets. We make the following assumptions to ensure the existence and uniqueness of a solution to the SDE.

Assumption 1. *The functions $f(x(t), \bar{u}(t))$ and $g(x(t), \bar{u}(t))$ are defined and measurable on $\mathcal{X} \times \mathcal{U}$.*

Assumption 2. *Equation (7) has a unique solution $x(t)$, which is continuous with probability 1, and $\exists$ a $K \in \mathbb{R}^{++}$ such that*

the following conditions are satisfied:
a) Lipschitz condition [35]: $\forall t \in [t_0, t_f]$, $s_1 \& s_2 \in \mathcal{X} \times \mathcal{U}$,

$$\|f(s_1) - f(s_2)\| + \|g(s_1) - g(s_2)\|_F \leq K\|s_1 - s_2\|, \quad (8)$$

b) Restriction on growth: $\forall t \in [t_0, t_f]$, $s_1 \in \mathcal{X} \times \mathcal{U}$

$$\|f(s_1)\|^2 + \|g(s_1)\|_F^2 \leq K^2(1 + \|s_1\|^2). \quad (9)$$

We use the following definition to study the controllability of the deterministic approximation of the SDE (7).

Definition 1. *The SDE (7) is ϵ_c-controllable [24]. For any initial state $x_0 \in \mathcal{X}$, we can compute a sequence of control $\bar{u}(t)$ $\forall t \in [t_0, t_f]$ such that* $\Pr\left(\|x - x(t_f)\|^2 \geq \delta \mid x(t_0) = x_0\right) \leq \epsilon_c$, *where $x(t_f)$ is the terminal state, $\delta > 0$ and $\epsilon_c > 0$ are small, and t_f is finite.*

Control Policy. We assume that the control policy $\bar{u}(t) \in \mathcal{U} \subseteq \mathbb{R}^{d_u}$ is deterministic and the set $\mathcal{U}$ is a convex set. The deterministic control policy is motivated by a hardware implementation strategy, where a state dependent Markov control policy defined on the compact set $\mathcal{X}$ is sampled for a value with highest probability (or) for the mean.
Note: We use the gPC method to project the SDE to an Ordinary Differential Equation (ODE) in a higher dimensional space for propagating the dynamics.

2) Chance Constraints [19]: In order to accommodate the unbounded uncertainty model in the dynamics, the feasible region $\mathcal{X}_{\mathcal{F}}$ defined as,

$$\mathcal{X}_{\mathcal{F}} = \{x(t) \in \mathcal{X} : h_i(x(t)) \leq 0 \ \forall \ i \ \in \ \{1, \ldots, m\}\}, \quad (10)$$

is relaxed to a chance constraint (CC) using the risk measure ϵ,

$$\mathcal{X}_{\mathrm{CC}} = \{x(t) \in \mathcal{X} : \Pr(x(t) \in \mathcal{X}_{\mathcal{F}}) \geq 1 - \epsilon\}, \quad (11)$$

with a guaranteed constraint satisfaction probability of $1 - \epsilon$. The constraint set $\mathcal{X}_{\mathcal{F}}$ is assumed to be the polytope $\mathcal{X}_{\mathcal{F}} = \{x \in \mathcal{X} : \wedge_{i=1}^m a_i^\top x + b_i \leq 0\}$ with m flat sides, or a quadratic constraint set $\mathcal{X}_{\mathcal{F}} = \{x \in \mathcal{X} : x^\top A x \leq c\}$ for any realization x of the state. The joint chance constraint formulation of the polytopic constraint is of the form, $\Pr(\wedge_{i=1}^m a_i^\top x + b_i \leq 0) \geq 1 - \epsilon$.

A convex relaxation of the individual chance constraint for an arbitrary distribution of the state vector $x(t)$ due to the nonlinearity in the system is intractable, so an extension of the problem called Distributionally-Robust Chance Constraints (DRCC) given as follows,

$$\mathcal{X}_{\mathrm{DRCC}} = \{x(t) \in \mathcal{X} : \inf_{x(t) \sim (\mu_x, \Sigma_x)} \Pr(x(t) \in \mathcal{X}_{\mathcal{F}}) \geq 1 - \epsilon\}, \quad (12)$$

where the chance constraint is satisfied for all distributions with known mean and variance of the decision variable is used. The set defined by the DRCC in (12) is a conservative approximation [20] of the chance constraint i.e., $\mathcal{X}_{\mathrm{DRCC}} \subseteq \mathcal{X}_{\mathrm{CC}}$.
a) *Distributionally-Robust Linear Chance Constraint (DRLCC) [19]:* Consider a single Linear Chance Constraint (LCC) with $a \in \mathbb{R}^{d_x}$ and $b \in \mathbb{R}$:

$$\mathcal{X}_{\mathrm{LCC}} = \{x(t) \in \mathcal{X} : \Pr(a^\top x(t) + b \leq 0) \geq 1 - \epsilon\}. \quad (13)$$

The column vector a, real constant b, and risk measure ϵ are known a priori. The state vector x is the decision variable. Assuming that the mean μ_x and the covariance Σ_x of x are known, a distributionally-robust constraint version of (13) is given as follows:

$$\mathcal{X}_{\mathrm{DRLCC}} = \{x(t) \in \mathcal{X} : \inf_{x(t) \sim (\mu_x, \Sigma_x)} \Pr(a^\top x(t) + b \leq 0) \geq 1 - \epsilon\}. \quad (14)$$

Equivalently, (14) can be rewritten in the following deterministic form, which will be used to derive a second-order cone constraint for the DNOC in Section III-E.

$$\mathcal{X}_{\mathrm{DRLCC}} = \{x(t) \in \mathcal{X} : a^\top \mu_x(t) + b + \sqrt{\frac{1-\epsilon}{\epsilon}} \sqrt{a^\top \Sigma_x a} \leq 0\} \quad (15)$$

Lemma 1. *The set $\mathcal{X}_{\mathrm{DRLCC}}$ in (15) is a subset of $\mathcal{X}_{\mathrm{LCC}}$ defined in (13).*

Proof: See Theorem 3.1 in [19]. ∎

If the dynamics are linear, the constraint in (15) is replaced with a tighter equivalent deterministic constraint given by the following inequality:

$$a^\top \mu_x(t) + b + \mathrm{erf}(1 - 2\epsilon)\sqrt{a^\top \Sigma_x a} \leq 0, \quad (16)$$

where the function erf(.) is defined as $\mathrm{erf}(\delta) = \frac{2}{\sqrt{\pi}} \int_0^\delta e^{-t^2} dt$ and $\forall \epsilon \in (0, 0.5)$. The constraint set is transformed to a second-order cone constraint in the gPC variables.

Remark 1. *The risk measure ϵ in (13) is assumed to be in the range $[0.001, 0.5]$. For small values of ϵ (< 0.001), the value $\sqrt{\frac{1-\epsilon}{\epsilon}}$ increases dramatically. This decreases the feasible space defined by the set $\mathcal{X}_{\mathrm{LCC}}$ drastically leading to numerical issues in the gPC-SCP method. For handling the risk of a very small value of ϵ (e.g., $1e - 7$, as discussed in [55]), the uncertainty in the system needs to be modeled accurately such that Σ_x is small or a newer deterministic surrogate method needs to be developed to overcome the numerical instability.*

b) *Conservative Quadratic Chance Constraint (CQCC):* Lemma 2 presents a new conservative deterministic relaxation for the quadratic chance constraint that is used to bound the deviation of the random vector $x(t)$ from the mean $\mu_x(t)$.

Lemma 2. *The constraint set*

$$\mathcal{X}_{\mathrm{CQCC}} = \{x(t) \in \mathcal{X} : \frac{1}{c} tr(A\Sigma_x) \leq \epsilon\} \quad (17)$$

is a conservative approximation of the original Quadratic Chance Constraint (QCC)

$$\mathcal{X}_{\mathrm{QCC}} = \{x \in \mathcal{X} : \Pr((x - \mu_x)^\top A(x - \mu_x) \geq c) \leq \epsilon\} \quad (18)$$

i.e., $\mathcal{X}_{\mathrm{CQCC}} \subseteq \mathcal{X}_{\mathrm{QCC}}$, where $A \in \mathbb{R}^{n \times n}$ is a positive definite matrix and $c \in \mathbb{R}^{++}$ and Σ_x is the covariance of the random variable x

Proof: See Proposition 1 in [1]. ∎

Corollary 1. *The constraint set $\frac{1}{c} tr(A\Sigma_x) + \frac{1}{c}(\mu_x^\top A\mu_x) \leq \epsilon$ is a conservative approximation of the quadratic chance constraint $\Pr(x^\top A x \geq c) \leq \epsilon$, where $A \in \mathbb{R}^{n \times n}$ is a positive*

definite matrix and $c \in \mathbb{R}^{++}$ and Σ_x is the co-variance of the random variable x.

Proof: The proof follows from Lemma 2. ∎

c) *Joint Chance Constraints (JCC)* [20]: The distributionally-robust joint chance constraint (DRJCC) for a polytope set is defined as $\inf_{x(t) \sim (\mu_x, \Sigma_x)} \Pr(\wedge_{i=1}^m a_i^\top x + b_i \leq 0) \geq 1 - \epsilon$. The joint constraints are split into multiple single chance constraints using Bonferroni's inequality [20] method as follows:

$$
\begin{aligned}
&\inf_{x(t) \sim (\mu_x, \Sigma_x)} \Pr(\wedge_{i=1}^m a_i^\top x + b_i \leq 0) \geq 1 - \epsilon \\
&\iff \sup_{x(t) \sim (\mu_x, \Sigma_x)} \Pr(\vee_{i=1}^m a_i^\top x + b_i \geq 0) \leq \epsilon \\
&\subseteq \sum_{i=1}^m \sup_{x(t) \sim (\mu_x, \Sigma_x)} \Pr(a_i^\top x + b_i \geq 0) \leq \epsilon.
\end{aligned}
\tag{19}
$$

If the probability distribution of x is Gaussian, then the JCC are split using Boole's inequality [2]. The total risk measure ϵ is allocated between each of the chance constraints in the summation such the $\sum_{i=1}^m \epsilon_i = \epsilon$ leading to m individual DRCC of the following form.

$$
\inf_{x(t) \sim (\mu_x, \Sigma_x)} \Pr(a_i^\top x + b_i \leq 0) \geq 1 - \epsilon_i
\tag{20}
$$

We follow a naive risk allocation approach by equally distributing the risk measure ϵ among the m constraints such that $\epsilon_i = \frac{\epsilon}{m}$. Alternatively, optimal risk allocation [56] can be achieved using iterative optimization techniques. Using distributional robustness, Problem 1 is reformulated to the following Problem 2.

Problem 2. *Distributionally-Robust Chance-Constrained Stochastic Nonlinear Optimal Control.*

$$
\begin{aligned}
J^*_{\text{DR-SNOC}} = \min_{x(t), \bar{u}(t)} \quad & \mathbb{E}\left[\int_{t_0}^{t_f} J(x(t), \bar{u}(t))dt + J_f(x(t_f)) \right] \\
\text{s.t.} \quad & (7), (15), (17), (4), and (5).
\end{aligned}
$$

Note: Given a risk measure ϵ, the constraints in Problem 2 are a function of mean μ_x and covariance matrix Σ_x of the state at any time t. While this enables fast computation of chance constraints, it reduces the feasible space $\mathcal{X}_F$. An optimal approach to trade off between the feasible space and computational complexity with theoretical guarantees seems infeasible due to the nonlinearity in the dynamics model. We present an empirical evidence that using distributional robustness approach does not lead to infeasibility in practical scenarios for both planning and control problems. For practical implementation, this approach should be integrated with system design to ensure feasibility. We will transform the SNOC problem to a DNOC problem by applying the generalized polynomial chaos expansion. This approach transforms the SNOC problem that is infinite dimensional in state (stochastic state) and time, to a problem that is infinite dimension only in time.

B. Generalized Polynomial Chaos ([15], [16], [52])

The generalized Polynomial Chaos (gPC) expansion theory is used to model uncertainty with finite second-order moments as a series expansion of orthogonal polynomials. The polynomials are orthogonal with respect to a known density function $\rho(.)$. Consider the random vector ξ with independent identically distributed (iid) random variables $\{\xi_i\}_{i=1}^{d_\xi}$ as elements. Each $\xi_i \sim \mathcal{N}(0, 1)$ is normally distributed with zero mean and unit variance. The random vector $x(t)$, defined by the SDE in (7) can be expressed as the following series

$$
x_i(t) = \sum_{j=0}^\infty x_{ij}(t)\phi_j(\xi),
\tag{21}
$$

where x_i denote the ith element in the vector $x \in \mathcal{X}$ and x_{ij} is the jth coefficient in the series expansion. The dimension d_ξ is the sum of number of random inputs in the SDE (7) and the number of random initial conditions. The functions $\phi_j(\xi)$ are constructed using the Hermite polynomial [15] basis functions. The functions $\phi_j(\xi)$ are orthogonal with respect to the joint probability density function $\boldsymbol{\rho}(\xi) = \varrho(\xi_1)\varrho(\xi_2) \cdots \varrho(\xi_{d_\xi})$, where $\varrho(\xi_k) = \frac{1}{\sqrt{2\pi}} e^{\frac{-\xi_k^2}{2}}$. The choice of the orthogonal polynomials depends on the uncertainty model effecting the dynamics. We refer to [17] for details on type and construction of the polynomials for different standard uncertainty models such as uniform, beta and Poisson distributions.

Remark 2. *The series expansion is truncated to a finite number $\ell + 1$ as $x_i \approx \sum_{j=0}^\ell x_{ij}(t)\phi_j(\xi)$ based on the maximum degree of the polynomials P_{gPC} required to represent the variable x. The minimum ℓ required to appropriately represent x with uncertainty parameter $\xi \in \mathbb{R}^{d_\xi}$ is given by $\ell = \binom{\mathrm{P}_{\text{gPC}} + d_\xi}{d_\xi} - 1$.*

The coefficients $x_{ij}(t)$ are computed using the Galerkin projection given by the following equation:

$$
x_{ij}(t) = \frac{\int_{\mathbb{D}} \boldsymbol{\rho}(\xi) x_i(t) \phi_j(\xi) d\xi}{\langle \phi_j(\xi), \phi_j(\xi) \rangle},
\tag{22}
$$

where $\langle \phi_i(\xi), \phi_j(\xi) \rangle = \int_{\mathbb{D}} \boldsymbol{\rho}(\xi) \phi_i(\xi) \phi_j(\xi) d\xi$. For non-polynomial functions, the Galerkin projection is computed using the Stochastic Collocation [16] method as follows:

$$
\int_{\mathbb{D}} \rho(\xi) x_i(t) \phi_j(\xi) d\xi \approx \sum_{k=1}^m w_k x_i(t) \phi_j(n_k),
\tag{23}
$$

where Gauss-Hermite quadrature is used to generate the nodes n_k and the corresponding node weights w_k. In the following section, we derive an approximate nonlinear ordinary differential equation system for the SDE in (7) using gPC expansion and the Galerkin scheme. The DRCC are projected to the gPC coordinates x_{ij} leading to convex constraints. Following Lemmas 3 and 4 discuss the convergence of the gPC expansion to the true distribution and the error due to truncated polynomial approximation of a distribution.

Lemma 3. *(Cameron-Martin Theorem [57]) The gPC series approximation in (21) converges to the true value $x_i \in \mathcal{L}_2$.*

$$
\|x_i(t) - \sum_{j=0}^\ell x_{ij}(t)\phi_j(\xi)\|_{\mathcal{L}_2} \to 0, \text{ as } \ell \to \infty \; \forall \, t \in [t_0, t_f]
\tag{24}
$$

Remark 3. *The expectation $\mathbb{E}(x_i)$ and variance Σ_{x_i} of the random variable x_i can be expressed in terms of the*
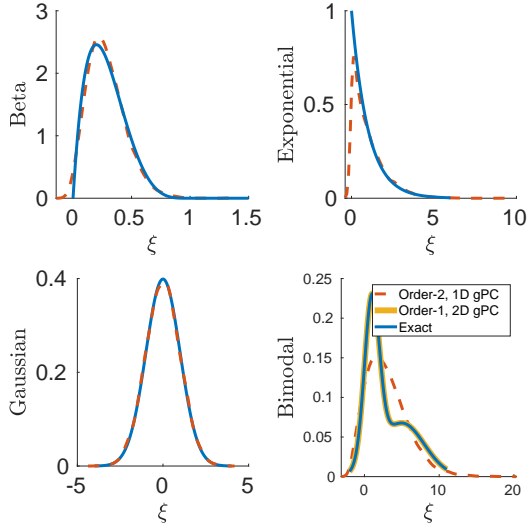
Fig. 2. Example gPC approximation of some standard probability distribution functions (PDF) using gPC expansion. For the beta and exponential distributions, gPC expansion represents the PDF well with just second order approximation. For a Gaussian distribution, the gPC representation is exact.

coefficients of the expansion as follows:

$$\mathbb{E}(x_i) = x_{i0}, \quad \Sigma_{x_i} \approx \sum_{j=1}^{\ell} x_{ij}^2 \langle \phi_j, \phi_j \rangle \text{ as } \ell \to \infty. \quad (25)$$

Lemma 4. *(Truncation Error Theorem [58]) If an element x_i of the random variable x is represented using ℓ polynomials, then the approximation error is given as follows:*

$$\left\| x_i - \sum_{j=0}^{\ell} x_{ij}(t)\phi_j(\xi) \right\| = \|e_\ell\| \le \sqrt{\sum_{j=\ell+1}^{\infty} x_{ij}^2 \|\phi_j\|^2}. \quad (26)$$

Lemmas 3 and 4, and Remark 3 will be used in studying the convergence of the gPC approximation of the cost function, the SDE, and the chance constraints. Furthermore, the higher-order moments can be expressed as a polynomial function of the coefficients.

Curse of Dimensionality: The truncated polynomial expansion is a finite-dimensional approximation of the random variable. The number of polynomials ℓ grow exponentially large based on the degree of polynomial used to represent the state distribution. The large dimensionality can be reduced, inducing sparsity in the gPC expansion, by using techniques like sparse gPC [59], and data-driven gPC [60]. A cost-effective approach to estimate moments up to second order is to use gPC polynomials up to degree 2, i.e., $P_{gPC} = 2$ [61]. The computationally complexity for $P_{gPC} = 2$ is equivalent to linear covariance propagation. Note that, unlike the linear covariance propagation method, the gPC method with $P_{gPC} = 2$ accounts for the coupling between the state x and the white-noise process dw.

III. DETERMINISTIC SURROGATE OF THE SNOC PROBLEM

The stochastic nonlinear optimal control problem discussed in Section II-A is reformulated in terms of the coefficients of the gPC expansion, with decision variables as the gPC coefficients and the control $\bar{u}$. In the following, we discuss the existence and uniqueness of a solution to the coupled Ordinary Differential Equations (ODE) obtained form gPC approximation of SDE, the cost function in the gPC space, and present the convex constraints for the gPC coefficients obtained from deterministic approximation of chance constraints. We present the convergence and feasibility theorem of the approximation at the end of this section.

A. Deterministic ODE Approximation of the SDE

The gPC expansion in (21) is applied for all the elements in the vector $x \in \mathcal{X} \subseteq \mathbb{R}^{d_x}$ and the matrix representation using Kronecker product is given in the following, where $\mathrm{X} = \begin{bmatrix} x_{10} & \cdots & x_{1\ell} & \cdots & x_{d_x 0} & \cdots & x_{d_x \ell} \end{bmatrix}^\top$ are gPC states.

$$\Phi(\xi) = \begin{bmatrix} \phi_0(\xi) & \cdots & \phi_\ell(\xi) \end{bmatrix}^\top \quad (27)$$

$$x \approx \bar{\Phi}\mathrm{X}; \text{ where } \bar{\Phi} = \mathbb{I}_{d_x \times d_x} \otimes \Phi(\xi)^\top \quad (28)$$

Consider the following Ito's integral form of the SDE in (7).

$$x(t) = x(t_0) + \int_{t_0}^{t} f(x, \bar{u})dt + \int_{t_0}^{t} g(x, \bar{u})dw \quad (29)$$

The gPC projection of the above SDE is given by the following ODE.

$$x_{ij}(t) = x_{ij}(t_0) + \int_{t_0}^{t} \bar{f}_{ij}(\mathrm{X}, \bar{u})dt + \int_{t_0}^{t} \bar{g}_{ij}(\mathrm{X}, \bar{u})\sqrt{dt} \quad (30)$$

$$\bar{f}_{ij} = \frac{\int_{\mathbb{D}} \rho(\xi)\phi_j(\xi)f_i(\bar{\Phi}\mathrm{X}, \bar{u})d\xi}{\langle \phi_j(\xi), \phi_j(\xi) \rangle},$$

$$\bar{g}_{ij} = \frac{\int_{\mathbb{D}} \rho(\xi)\phi_j(\xi)g_i(\bar{\Phi}\mathrm{X}, \bar{u})\xi d\xi}{\langle \phi_j(\xi), \phi_j(\xi) \rangle}$$

The dynamics of the coefficients x_{ij} with the above notation is given in (32), where: f_i and g_i are the ith element of the vector f and i^{th} row of the matrix g respectively. We use the Euler-Maruyama discretization method of the SDE for time integration. The discrete time stochastic dynamics is given as follows:

$$x[k+1] = x[k] + f(x[k], \bar{u}[k])\Delta t + g(x[k], \bar{u}[k])\sqrt{\Delta t}\xi, \quad (31)$$

where $x[k]$, $\bar{u}[k]$ are the states and controls at time step k, Δt is the integration time interval, and ξ is a multivariate Gaussian distribution $\mathcal{N}(0, \mathbb{I})$. The discrete stochastic system is projected to a discrete deterministic system using the gPC method.

$$\begin{aligned} x_{ij}[k+1] = x_{ij}[k] &+ \bar{f}_{ij}(\mathrm{X}[k], \bar{u}[k])\Delta t \\ &+ \bar{g}_{ij}(\mathrm{X}[k], \bar{u}[k])\sqrt{\Delta t} \end{aligned} \quad (32)$$

The full nonlinear discrete time ODE with the stacked vector X is given as follows:

$$\begin{aligned} \mathrm{X}[k+1] = &\mathrm{X}[k] + \bar{f}(\mathrm{X}[k], \bar{u}[k], \Delta t) \\ &+ \bar{g}(\mathrm{X}[k], \bar{u}[k], \sqrt{\Delta t}). \end{aligned} \quad (33)$$

Figure 3 shows an example of propagation using (33). While not discussed in this paper, the projection is also applicable to a higher-order discretization methods [62]. The sequential
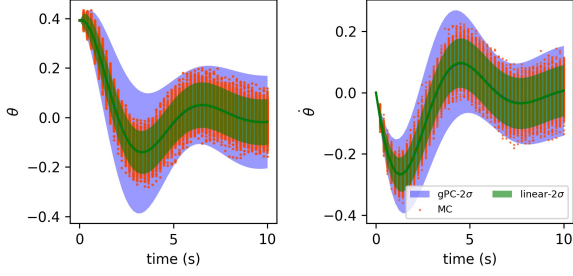
Fig. 3. Example gPC propagation for a pendulum. The figure compares the mean and 2σ confidence computed using gPC Projection ($P_{\mathrm{gPC}} = 1$), linear covariance propagation, and Monte Carlo (MC) propagation of the simple pendulum dynamics $\ddot{\theta} = -\sin\theta - 0.8\dot{\theta} + \sqrt{0.001}\xi(t)$. It is observed that the gPC approximation overestimates the variance compared to MC and the linear covariance propagation underestimates the variance. The $P_{\mathrm{gPC}} = 1$ projection corresponds to a Gaussian approximation that includes the cross correlation between the state and uncertainty.

convex programming method used for trajectory optimization involves successive linearizations [21] of the dynamics about a given trajectory and discretization for time integration. In Proposition 1, we present the conditions for existence and uniqueness of the solution to the projected system. The existence and uniqueness of solution to the ODE surrogate ensure convergence of any Picard iteration scheme used for integration.

Proposition 1. *The ODE system (32) obtained using gPC approximation of the SDE has a solution and the solution is unique, for a given initial condition, assuming that the SDE satisfies the existence and uniqueness conditions in (8), (9) and the expectation*

$$K_{g_{ij}} = \frac{K}{k_j}\mathbb{E}(L_{g_j}(\xi)), K_{f_j} = \frac{K}{k_j}\mathbb{E}(L_{f_j}(\xi)) \qquad (34)$$

in (34) are bounded for each $j = 0, 1, \cdots, \ell$, where: $P = \begin{bmatrix} \bar{\Phi} & 0 \\ 0 & \mathbb{I} \end{bmatrix}$, $k_j = \langle \phi_j, \phi_j \rangle$, $L_{f_j}(\xi) = |\phi_j(\xi)| \|P\|_2$, $L_{g_j}(\xi) = L_{f_j}(\xi)|\phi_1(\xi)|$. The constants $K_{g_{ij}}$ and K_{f_j} are the Lipschitz coefficients of the projected functions $\bar{g}_{ij}$ and $\bar{f}_j$ respectively.

Proof: See Proposition 1 of [1]. ∎

While the projection operation preserves the existence and uniqueness properties of the SDE, it might not conserve the controllability of the moments of the system. Following examples discuss on how the ϵ_c controllability in Definition 1 of the SDE effects the controllablility of the projected ODE system.

Example 1. *Consider the linear SDE $dx = xdt + \bar{u}dt + \sqrt{dt}\xi$, where $x \in \mathbb{R}^1$, $\bar{u} \in \mathbb{R}^1$ and $\xi \sim \mathcal{N}(0, 1)$. Using the random variable ξ as the variable, we can construct the first order gPC expansion $x = x_0 + x_1\xi$ of the state with $x_0, x_1 \in \mathbb{R}^1$. The projected dynamics using the expansion is given as follows:*

$$\begin{bmatrix} dx_0 \\ dx_1 \end{bmatrix} = \begin{bmatrix} 1 & 0 \\ 0 & 1 \end{bmatrix}\begin{bmatrix} x_0 \\ x_1 \end{bmatrix} dt + \begin{bmatrix} 1 \\ 0 \end{bmatrix}\bar{u}dt + \begin{bmatrix} 0 \\ \sqrt{dt} \end{bmatrix}. \qquad (35)$$

The dynamics of x_1 is decoupled from x_0 and the propagation is not influenced by the control $\bar{u}$. Notice that, even though the original SDE ($dx = xdt + \bar{u}dt$) is controllable, the projected

system (35) is not fully controllable. The projection operation converts a SDE to an ODE in higher dimensions. Though this operation enables for fast uncertainty propagation, the linear projected system is underactuated and not fully controllable.

Remark 4. *Using a stochastic state feedback of the form $u = -kx$ in Example 1, we get the closed-loop SDE $dx = (1 - k)xdt + \sqrt{dt}\xi$. The gPC projection of the system is as follows:*

$$\begin{bmatrix} dx_0 \\ dx_1 \end{bmatrix} = \begin{bmatrix} 1 - k & 0 \\ 0 & 1 - k \end{bmatrix}\begin{bmatrix} x_0 \\ x_1 \end{bmatrix} dt + \begin{bmatrix} 0 \\ \sqrt{dt} \end{bmatrix}. \qquad (36)$$

Using a stochastic feedback, the state x_1 that corresponds to the variance of the SDE can be controlled.

Example 2. *The gPC projection of the nonlinear SDE $dx = x^2 dt + \sqrt{dt}\xi$ using the expansion $x = x_0 + x_1\xi$ is given as follows:*

$$\begin{bmatrix} dx_0 \\ dx_1 \end{bmatrix} = \begin{bmatrix} x_0^2 + x_1^2 + \bar{u} \\ 2x_0 x_1 \end{bmatrix} dt + \begin{bmatrix} 0 \\ \sqrt{dt} \end{bmatrix}. \qquad (37)$$

The projected system (37) is underactuated. In the case of nonlinear systems, the coupling between the dynamics of x_0 and x_1 allows for indirectly controlling the state x_1.

Remark 5. *The gPC projected ODE system in (32) might not be fully controllable as discussed in Example 1. We choose soft terminal constraints on the variance of the state variable to ensure the feasibility of Problem 1 in accordance with Definition 1.*

With Remark 5 on the controllability of the projected system, we proceed to construct a finite-dimensional approximation of the cost functional and chance-constraints to formulate the convex-constrained nonlinear deterministic optimal control problem.

B. Cost Function

Using the notation in (28), the expectation of the cost functional in (6) is expressed in the gPC coefficients as follows:

$$\begin{aligned} J_{\mathrm{gPC}}(X(t), \bar{u}(t)) &= X(t)^\top Q_{\mathrm{gPC}}X(t) + \|\bar{u}\|_p, \\ J_{\mathrm{gPC}_f}(X(t_f)) &= X(t_f)^\top Q_{\mathrm{gPC}_f}X(t_f), \end{aligned} \qquad (38)$$

where $Q_{\mathrm{gPC}} = \mathbb{E}(\bar{\Phi}^\top Q\bar{\Phi})$ and $Q_{\mathrm{gPC}_f} = \mathbb{E}(\bar{\Phi}^\top Q_f\bar{\Phi})$. Since the gPC projection is a canonical transformation, we can prove that the projected matrix Q_{gPC} is positive definite.

Proposition 2. *The expectation matrix $\mathbb{E}(\bar{\Phi}^\top\bar{\Phi})$ is a positive definite matrix.*

Proof: We can prove the following equality by expanding the matrix multiplication.

$$\mathbb{E}(\bar{\Phi}^\top\bar{\Phi}) = \mathbb{I} \otimes \mathbb{E}(\Phi\Phi^\top) \qquad (39)$$

The block matrix $\mathbb{E}(\Phi\Phi^\top)$ is positive definite as the functions ϕ_i used to construct the column vector Φ are orthogonal with respect to the density function ρ. Therefore, $\mathbb{E}(\bar{\Phi}^\top\bar{\Phi})$ is positive definite, since $\mathbb{E}(\Phi\Phi^\top)$ is positive definite. ∎

Lemma 5. *If Q is a positive definite matrix, then the expectation $Q_{\mathrm{gPC}} = \mathbb{E}(\bar{\Phi}^\top Q\bar{\Phi})$ is a positive definite matrix.*

Proof: Since Q is a positive definite matrix, we have $Q \succcurlyeq \lambda_{\min}(Q)\mathbb{I}$ where $\lambda_{\min}(Q) > 0$. The expectation $\mathbb{E}(\bar{\Phi}^\top Q \bar{\Phi})$ can be lower bounded as follows:

$$\mathbb{E}(\bar{\Phi}^\top Q \bar{\Phi}) \succcurlyeq \mathbb{E}(\bar{\Phi}^\top \lambda_{\min}(Q)\mathbb{I}\bar{\Phi}), \tag{40}$$

$$\succcurlyeq \lambda_{\min}(Q).\mathbb{E}(\bar{\Phi}^\top \bar{\Phi}) \tag{41}$$

Using Proposition 2 in (41), we conclude that $\mathbb{E}(\bar{\Phi}^\top Q \bar{\Phi})$ is a positive definite matrix. ∎

Corollary 2. *If the polynomials ϕ_i used for gPC projection are Hermite polynomials, then $\mathbb{E}(\bar{\Phi}^\top Q \bar{\Phi}) \succcurlyeq \lambda_{\min}(Q)\mathbb{I}$.*

Proof: We can prove Corollary 2 by using the fact that for Hermite polynomials $\mathbb{E}(\bar{\Phi}^\top \bar{\Phi}) \succcurlyeq \mathbb{I}$ in Lemma 5. ∎

C. Convex Approximation of the Chance Constraint

The deterministic approximations of the chance constraints discussed in Section II-A are expressed in terms of the gPC coefficients that define a feasible set for the deterministic optimal control problem with gPC coefficients as decision variables.

Lemma 6. *The second-order cone constraint given below*

$$(a^\top \otimes M)\mathrm{X} + b + \sqrt{\frac{1-\epsilon}{\epsilon}}\sqrt{\mathrm{X}^\top U N N^\top U^\top \mathrm{X}} \leq 0 \tag{42}$$

is equivalent to the deterministic approximation of the DRLCC in (14) as $\ell \to \infty$., where the matrices M, U, N are given by

$$M = \begin{bmatrix} 1 & 0 & \cdots & 0 \end{bmatrix}_{1 \times (\ell+1)}$$

$$U = \begin{bmatrix} a_1 & 0 & 0 \\ 0 & \ddots & 0 \\ 0 & 0 & a_{d_x} \end{bmatrix} \otimes \mathbb{I}_{(\ell+1) \times (\ell+1)}$$

$$N = \mathbb{1}_{d_x \times d_x} \otimes \mathbb{H}; \ \mathbb{H} = \begin{bmatrix} 0 & \mathbb{O} \\ \mathbb{O} & \sqrt{\mathbb{E}(HH^\top)} \end{bmatrix}$$

$$\text{where } H = \begin{bmatrix} \phi_1(\xi) & \cdots & \phi_\ell(\xi) \end{bmatrix}^\top$$

and $\mathbb{1}$ is a matrix with entries as 1.

Proof: It is sufficient to prove that $(a^\top \otimes M) \approx a^\top \mu_x$ and $\mathrm{X}^\top U N N^\top U^\top \mathrm{X} \approx a^\top \Sigma_x a$ as $\ell \to \infty$. Invoking Lemma 3 and Remark 3, the polynomials of gPC coefficients can be replaced by mean and variable of the variable x.

$$(a^\top \otimes M)\mathrm{X} = \begin{bmatrix} a_1 M & a_2 M & \cdots & a_{d_x} M \end{bmatrix} \mathrm{X}$$
$$= a_1 x_{10} + a_2 x_{20} + \cdots + a_{d_x} x_{dx0} \tag{44}$$
$$\approx a^\top \mu_x$$

Equation (44) shows the steps involved to prove $(a^\top \otimes M) \approx a^\top \mu_x$. Let us define a vector $p_i = \begin{bmatrix} x_{i0} & \bar{p}_i^\top \end{bmatrix}^\top$ where $\bar{p}_i = \begin{bmatrix} x_{i1} & \cdots & x_{i\ell} \end{bmatrix}^\top$.

$$U^\top \mathrm{X} = \begin{bmatrix} a_1 p_1^\top & a_2 p_2^\top & \cdots & a_{d_x} p_{d_x}^\top \end{bmatrix}^\top \tag{45}$$
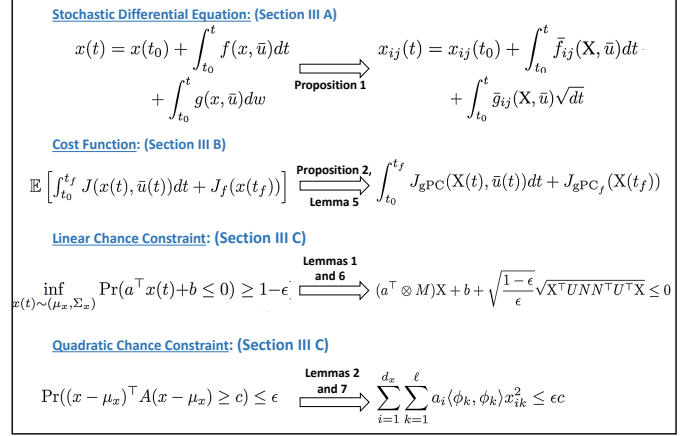

Fig. 4. Illustration of the gPC projection method. We use the gPC projection method to derive a deterministic surrogate of the chance-constrained optimal control problem. We use Lemmas 1 to 7 and Propositions 1 and 2 to prove Theorem 1.

$$N N^\top U^\top \mathrm{X} = \begin{bmatrix} \mathbb{H} a_1 p_1 & \mathbb{H} a_2 p_2 & \cdots & \mathbb{H} a_{d_x} p_{d_x} \end{bmatrix} \tag{46}$$

$$\mathrm{X}^\top U N N^\top U^\top X = \sum_{i=1}^{d_x} \sum_{j=1}^{d_x} a_i a_j p_i^\top \mathbb{H} p_j \tag{47}$$

$$= \sum_{i=1}^{d_x} \sum_{j=1}^{d_x} a_i a_j \bar{p}_i^\top \mathbb{E}(HH^\top)\bar{p}_j \approx a^\top \Sigma_x a$$

Using this notation, the matrices in (42) are expanded as shown in (45), (46), and (47). Therefore the equivalence is proved by Lemma 3 as $\ell \to \infty$. ∎

Lemma 7. *The quadratic inequality*

$$\sum_{i=1}^{d_x} \sum_{k=1}^{\ell} a_i \langle \phi_k, \phi_k \rangle x_{ik}^2 \leq \epsilon c, \tag{48}$$

expressed in terms of the gPC coefficients is equivalent to the constraint in (17) as $\ell \to \infty$, where A is a diagonal matrix with i^{th} diagonal element as a_i and $\langle \phi_k, \phi_k \rangle = \int_{\mathbb{D}} \rho(\xi)\phi_k\phi_k d\xi$.

Proof: The deterministic approximation, $\mathrm{tr}(A\Sigma_x) \leq c\epsilon$, of the QCC in (18) can be expand as follows.

$$\mathrm{tr}(A\Sigma_x) \leq c\epsilon \equiv \sum_{i=1}^{d_x} a_i \mathbb{E}((x_i - \hat{x}_i)^\top (x_i - \hat{x}_i)) \leq c\epsilon$$
$$\equiv \sum_{i=1}^{d_x} \sum_{j=1}^{\ell} a_i \langle \phi_j, \phi_j \rangle x_{ij}^2 \leq c\epsilon \tag{49}$$

The equivalence is proved by directly expanding the trace and using Remark 3 as shown in (49). ∎

Using the projected dynamics (30), the cost functional in (38), and the linear and quadratic chance constraints (42), (48) in gPC coefficients (as shown in Fig. 4) we can formulate the following distributionally-robust deterministic nonlinear optimal control problem with the gPC states X and the control $\bar{u}$ as the decision variables.

Problem 3. *Distributionally-Robust Deterministic Nonlinear Optimal Control Problem.*

$$J_{\mathrm{gPC}}^* = \min_{\mathrm{gPC} \mathrm{X}(t), \bar{u}(t)} \int_{t_0}^{t_f} J_{\mathrm{gPC}}(\mathrm{X}(t), \bar{u}(t)) dt + J_{\mathrm{gPC}_f}(\mathrm{X}(t_f))$$

$$s.t. \qquad (33), \ (42), \ (48)$$

$$\bar{u}(t) \in \mathcal{U} \quad \forall t \in [t_0, t_f]$$

$$\mathrm{X}(t_0) = \mathrm{X}_0 \quad \mathrm{X}(t_f) \in \mathcal{X}_{\mathrm{X}_f}$$

where the projection of the initial condition x_0 in gPC space is X_0. The terminal set $\mathcal{X}_{\mathrm{X}_f}$ is constructed using a distributionally-robust polytope (or) a conservative ellipsoid approximation of the set x_f in Problem 1 with probabilistic guarantees using Lemmas 6 and 7. We make the following observations about distributional robustness and gPC projection discussed above for transforming Problem 1 to Problem 3.

- The infinite-dimensional optimal control problem in state space and time, as described in Problem 1, is projected to Problem 3, that is finite dimensional in space and infinite-dimensional in time.
- The ODE approximation of the SDE using gPC projection diverges over long horizon problem, (or) when the uncertainty effecting the SDE has large variance, (or) when the uncertainty model has large gradients with respect to state and control. A multi-element gPC method can be used to over come this divergence due to finite dimensional approximation. The structure of the proposed constraint reformulation is invariant to the multi-element gPC method.
- The choice of the terminal set used in Problem 1 is restricted due to the ϵ_c−controllability of the SDE. We use soft constraints on the terminal state to ensure the feasibility of both Problem 1 and 3.
- The projected cost functional preserves the positive definite property of the quadratic cost used in Problem 1.
- The linear and quadratic chance constraints for a given risk measure are second-order cone and semi definite constraints respectively in the gPC coefficients.

Problem 3 (DNOC) enables the use of techniques like psuedo-spectral method, and sequential convex programming for solving Problem 3 (SNOC). We use sequential convex programming to solve Problem 3 and apply this technique to compute safe and optimal motion plans under uncertainty. The model predictive extension of gPC-SCP is applied for controlling a nonlinear robotic system under uncertainty and safety constraints.

D. gPC-SCP: Generalized Polynomial Chaos-Based Sequential Convex Programming

We formulate the gPC-SCP problem by constructing a sequential convex programming (SCP) approximation of Problem 3 with gPC state (X) and control ($\bar{u}$) as the decision variables. The convex program is then solved iteratively using an interior point method till a convergence criteria is satisfied and projected back to the probability space from the gPC space to compute a solution of Problem 2.

The SCP problem formulation involves two steps: 1) Discretizing the continuous time optimal control problem to a discrete time optimal control problem, and 2) Convexifing the non-convex constraints and cost function about a nominal initial state and control trajectory. Following this approach, the projected integral cost functional (38), the nonlinear dynamics (33), and the second-order cone constraint (42) and semi-definite constraint (48) are discretized using a first-order hold approach for T time steps between the time horizon $[t_0, t_f]$ with gPC state and control as the decision variables.

At iteration i, the cost functional, constraints (42) and (48), and feasible control set $\mathcal{U}$ are convex. The discretized gPC dynamics in (33) is a nonlinear equality constraint at each time step. We convexify the nonlinear dynamics (33) by linearizing it about the state and control trajectory $S^{(i-1)} = \{\mathrm{X}^{(i-1)}, \bar{u}^{(i-1)}\}$ computed at $(i-1)^{th}$ iteration. The linearized equations form a set of linear constraints on the state and control action as follows:

$$\mathrm{X}^{(i)}[k+1] = \mathrm{X}^{(i)}[k] + A^{(i)}[k]\mathrm{X}^{(i)}[k] + B^{(i)}[k]\bar{u}^{(i)}[k]$$
$$+ Z^{(i)}[k], \quad \text{where} : k \in \{1, \ldots, T-1\}. \tag{50}$$

$$A^{(i)} = \frac{\partial(\bar{f} + \bar{g})}{\partial \mathrm{X}}\Big|_{S^{(i-1)}}; \quad B^{(i)} = \frac{\partial(\bar{f} + \bar{g})}{\partial \bar{u}}\Big|_{S^{(i-1)}}$$

$$Z^{(i)} = \bar{f}(S^{(i-1)}, \Delta t) + \bar{g}(S^{(i-1)}, \sqrt{\Delta t})$$
$$- A^{(i)}\mathrm{X}^{(i-1)} - B^{(i)}\bar{u}^{(i-1)} \tag{51}$$

The gPC-SCP problem at iteration i, after discretization and convexification is given in the following Problem 4.

Problem 4. *gPC-SCP: Generalized Polynomial Chaos-based Sequential Convex Programming.*

$$\min_{\mathrm{X}^{(i)}, \bar{u}^{(i)}} \sum_{k=1}^{T-1} J_{\mathrm{gPC}}(\mathrm{X}^{(i)}[k], \bar{u}^{(i)}[k])\Delta t + J_{\mathrm{gPC}_f}(\mathrm{X}^{(i)}[T])$$

$$s.t. \qquad \text{Projected Dynamics} : (50)$$

$$\text{Constraints} : \{(42), \ (48)\}$$

$$\bar{u}^{(i)}[k] \in \mathcal{U} \quad \forall \ k \in \{1, \cdots, T-1\}$$

$$\mathrm{X}^{(i)}[1] = \mathrm{X}_0 \quad \mathrm{X}^{(i)}[T] \in \mathcal{X}_{\mathrm{X}_f}$$

$$\|\mathrm{X}^{(i)}[k] - \mathrm{X}^{(i-1)}[k]\|_2^2 \le \alpha_x \beta \ \forall \ k \in \{1, \ldots, T\} \tag{52}$$

$$\|\bar{u}^{(i)}[k] - \bar{u}^{(i-1)}[k]\|_2^2 \le \alpha_u \beta \ \forall \ k \in \{1, \ldots, T-1\} \tag{53}$$

Problem 4 shows the SCP formulation at i^{th}, given a nominal trajectory $S^{(i-1)} = \{\mathrm{X}^{(i-1)}, \bar{u}^{(i-1)}\}$ computed at $(i-1)^{\mathrm{th}}$ iteration with the constraint set at each time step k and iteration i, where $\mathcal{X}_{\mathrm{X}_f}$ is the projected terminal constraint. The nominal trajectory S^0 at $i = 1$, used to initialize gPC-SCP, is computed using a deterministic trajectory optimization for the nominal dynamics $\dot{x} = f(x, \bar{u})$, that ignores the uncertainty affecting the system. For motion planning problem, the nominal trajectory S^0 is computed using kino-dynamic motion planning algorithms like asymptotically-optimal rapidly exploring random trees [26].

An additional trust region constraint on the gPC state (52) and control (53) are used to ensure the convergence and feasibility of the SCP as $i \to \infty$, where $\alpha_x > 0$, $\alpha_x > 0$, and $\beta \in (0, 1)$. The choice of β ensures the convergence of the trust region as the number of iterations increases. This

acts as a convergence criteria, while ensuring that the search space is small. The trust region on gPC state in (52) can be equivalently understood as probabilistic constraint of the form $\Pr(\|x^i - x^{i-1}\| \leq \alpha_{xp}) \geq 1 - \epsilon_t$, where α_x is a function of α_{xp} using the quadratic projection discussed in Lemma 7. The SCP algorithm is known to converge to the KKT point of the DNOC problem under mild conditions. For detailed analysis on convergence, see [21]–[23]. We ensure feasibility of gPC-SCP: 1) by using stochastic reachable terminal sets, as discussed in [39], that are constructed using the linearized approximation of the dynamics, and 2) by increasing the trust region in-loop with $\beta > 1$ when infeasibility occurs.

E. Sub-Optimality and Convergence

In this subsection, we study the optimality of Problem 3 and show that Problem 3 computes a sub-optimal solution to Problem 1. We make a two step approximation of Problem 1 by using distributional robustness to formulate Problem 2 with known mean and variance of the state and then use gPC propagation to construct the deterministic optimal control Problem 3 that is solved using SCP. In Lemma 8, we prove the sub-optimality of the optimal cost J^*_{SNOC} of Problem 1 compared to the optimal cost $J^*_{\mathrm{DR-SNOC}}$ of Problem 2 that is distributionally robust.

Lemma 8. *The optimal solution of Problem 2 is a sub-optimal solution of Problem 1, i.e., $J^*_{\mathrm{SNOC}} \leq J^*_{\mathrm{DR-SNOC}}$.*

Proof: The constraint set $\mathcal{X}_{\mathrm{DRLCC}}$ and $\mathcal{X}_{\mathrm{CQCC}}$ in Problem 2 are a subset of the constraint set $\mathcal{X}_{\mathrm{LCC}}$ and $\mathcal{X}_{\mathrm{QCC}}$ of Problem 1 respectively. Therefore, $J^*_{\mathrm{SNOC}} \leq J^*_{\mathrm{DR-SNOC}}$ as the feasible space of Problem 1 is larger than the feasible space of Problem 2. ∎

Problem 3 (DNOC) computed via gPC projection converges asymptotically to Problem 2 (SNOC). The following theorem discuss the conditions for convergence.

Theorem 1. *The surrogate deterministic nonlinear optimal control Problem 3 with convex constraints is a sub-optimal surrogate for the stochastic nonlinear optimal control Problem 1 with following being true:*
(a) In the case with no chance constraints, the cost $|J^*_{\mathrm{gPC}} - J^*| \to 0$ as $\ell \to \infty$
(b) In the case with linear and quadratic chance constraints, any feasible solution of Problem 3 is a feasible solution of Problem 1 as $\ell \to \infty$ and $J^*_{\mathrm{SNOC}} \leq J^*_{\mathrm{gPC}}$, assuming that a feasible solution exists.

Proof: **Case (a)**: It is sufficient to prove that the cost function and the dynamics are exact as $\ell \to \infty$. Using the Kronecker product notation, due to Lemma 3, we have the following

$$\|x - \bar{\Phi} \mathrm{X}\|_{\mathcal{L}_2} \to 0 \text{ as } \ell \to \infty \tag{54}$$

$$(54) \implies \|\dot{x} \to \bar{\Phi} \dot{\mathrm{X}}\|_{\mathcal{L}_2} \to 0 \text{ as } \ell \to \infty \tag{55}$$

$$(54) \implies |J_{\mathrm{gPC}} - J| \to 0 \text{ as } \ell \to \infty \\ |J_{\mathrm{gPC}_f} - J_f| \to 0 \text{ as } \ell \to \infty \tag{56}$$

From (55), and (56) we conclude that the optimal value $|J^*_{\mathrm{gPC}} - J^*| \to 0$ as $\ell \to \infty$, since the cost function, the

dynamics and the initial and terminal conditions converge to the original stochastic formulation (Problem 1) as $\ell \to \infty$.
Case (b): Consider the sets $\mathcal{X}_{\mathrm{LgPC}}$, and $\mathcal{X}_{\mathrm{QgPC}}$ defined below.

$$\mathcal{X}_{\mathrm{LgPc}} = \{x \in \mathcal{X} : x \approx \bar{\Phi} \mathrm{X} \text{ where X} \in \text{(42)}\} \tag{57}$$

$$\mathcal{X}_{\mathrm{QgPC}} = \{x \in \mathcal{X} : x \approx \bar{\Phi} \mathrm{X} \text{ where X} \in \text{(48)}\} \tag{58}$$

Using Lemmas 6 and 7, we have the approximate convex constraints converge to the deterministic equivalent of the distributionally robust chance constraint as $\ell \to \infty$.

$$\begin{aligned} Lemma\ 6 \implies \mathcal{X}_{\mathrm{LgPc}} \to \mathcal{X}_{\mathrm{DRLCC}} \text{ as } \ell \to \infty \\ Lemma\ 7 \implies \mathcal{X}_{\mathrm{QgPC}} \to \mathcal{X}_{\mathrm{CQCC}} \text{ as } \ell \to \infty \end{aligned} \tag{59}$$

Using Lemmas 1 and 2, we have the following:

$$\begin{aligned} Lemma\ 1 \implies \mathcal{X}_{\mathrm{DRLCC}} \subseteq \mathcal{X}_{\mathrm{LCC}} \\ Lemma\ 2 \implies \mathcal{X}_{\mathrm{CQCC}} \subseteq \mathcal{X}_{\mathrm{QCC}} \end{aligned} \tag{60}$$

$$\{(59),\ (60)\} \implies \begin{cases} \mathcal{X}_{\mathrm{LgPc}} \subseteq \mathcal{X}_{\mathrm{LCC}} \text{ as } \ell \to \infty \\ \mathcal{X}_{\mathrm{QgPC}} \subseteq \mathcal{X}_{\mathrm{QCC}} \text{ as } \ell \to \infty \end{cases} \tag{61}$$

Combining (59) and (60), we can conclude that (61) holds as $\ell \to \infty$. In Fig. 4, we illustrate the Lemmas 1, 2, 6 and 7 used in proving this theorem. This proves that if a feasible solution exists for Problem 3 then it is a feasible solution of Problem 1 as $\ell \to \infty$. Using Lemma 8, as $\ell \to \infty$ we have $J^*_{\mathrm{gPC}} \to J^*_{\mathrm{DR-SNOC}}$. This implies that $J^*_{\mathrm{SNOC}} \leq J^*_{\mathrm{gPC}}$. ∎

The above theorem proves the consistency of the gPC projection method as $\ell \to \infty$. The asymptotic convergence of the cost and the chance constraints constraints is achieved with large number of the polynomials ϕ. This leads to a deterministic optimal control problem with size ℓd_x. The choice of ℓ depends on the number of uncertainty in the system and the nature of the state distribution. A computationally efficient approach is to use $P_{\mathrm{gPC}} = 2$ for generating the functions ϕ used in the projection. This replicates the computational efficiency of linear covariance propagation techniques, while ensuring the convexity of the chance constraints in gPC space. We study the chance constraint formulation for collision checking under uncertainty in dynamics and obstacle locations in the following section using distributional robustness and gPC projection.

IV. MOTION PLANNING UNDER UNCERTAINTY

The gPC-SCP method is applied for planning a safe trajectory under uncertain obstacles and for controlling a nonlinear dynamical system under uncertainty. We formulate the motion planning problem to incorporate uncertainty in dynamics and then show that deterministic projections of chance constraints in the gPC space enable convex formulations of the collision constraint for obstacles with both deterministic and stochastic state models.

The motion planning problem is to compute an optimal and safe trajectory ($x \in \mathcal{X}_{\mathcal{F}}$) for the SDE in (7) from an initial state $x_0 \in \mathcal{X}$ to the terminal set $\mathcal{X}_f \subseteq \mathcal{X}$ on a given map with static obstacles. In the following, we derive a chance constraint formulation of the collision constraint and terminal state constraint. The chance constraints are used to formulate
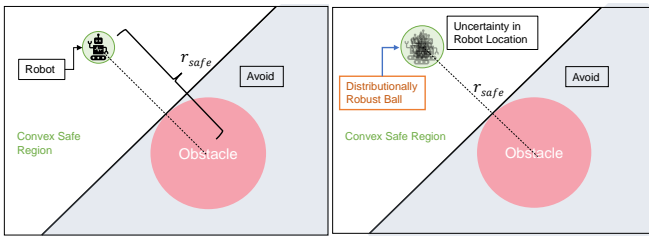
Fig. 5. An illustration of the convex linear constraint used for collision checking in deterministic SCP at a particular instant in time is shown on the left. The linear chance constraint under stochastic dynamics is projected to gPC space forming a second-order cone constraint. The cone constraint is visualized as a robustness bound on the robot's state as shown in the figure on right.

a SNOC problem as described in Problem 1. The SNOC problem is then projected to the gPC space for solving via the SCP method. At each SCP iteration, the collision constraints are approximated as linear chance constraint around the nominal trajectory and form a second-order cone constraint in gPC state X as discussed in Lemma 6. The terminal set is defined as a soft constraint on an ellipsoidal set and forms a semi-definite constraint in gPC states as discussed in Lemma 7.

In the following, we first discuss the linear chance constraint formulation for collision checking with a deterministic obstacle and then extend it to include the uncertainty in obstacle locations for SCP. We prove that the approximation is a subset of the original nonlinear chance constraint. We then discuss the chance constraint formulation of the terminal set constraint. The chance constraint formulations for collision checking and terminal set are used to design the motion planning algorithm that integrates an asymptotically-optimal sampling based planner [26] with the gPC-SCP Problem 4 for computing a safe trajectory under uncertainty.

A. Collision Checking with Deterministic Obstacles

We derive a second-order cone constraint approximation of the circular obstacle in the gPC coordinates under the uncertainty in dynamics at any point in time $t \in [t_0, t_f]$. The approximation involves two steps. We first derive a conservative linear chance constraint approximation of the nonlinear collision chance constraint. In the second step we project the linear chance constraint to a second order cone constraint in the gPC coordinates. Let the state of the obstacle be $\bar{p}_{\mathrm{obs}}$ at time t and the radius of the obstacle be r_{obs}. The collision chance constraint at any time t for a robot with the state distribution x and radius r_{rob} is given as follows:

$$\Pr\left(\|\mathbf{C}(x - \bar{p}_{\mathrm{obs}})\|_2 \geq r_{\mathrm{rob}} + r_{\mathrm{obs}}\right) \geq 1 - \epsilon_{\mathrm{col}}, \quad (62)$$

where the matrix $\mathbf{C}$ is used to compute the position of the obstacle and the robot given the states $\bar{p}_{\mathrm{obs}}$ and x respectively. The probability of collision is tuned using the risk measure $\epsilon_{\mathrm{col}} \in [0.001, 0.1]$. In the following theorem, we prove that, given a nominal state distribution trajectory x_{nom}, we can compute a conservative linear chance constraint approximation of the collision constraint (62). The nominal trajectory x_{nom} can computed by using a deterministic planner without considering the uncertainty in the dynamics.

Theorem 2. *The linear chance constraint,*

$$\Pr\Big((\bar{x}_{\mathrm{nom}} - \bar{p}_{\mathrm{obs}})^\top \mathbf{C}^\top \mathbf{C}(x - \bar{p}_{\mathrm{obs}})$$
$$\geq r_{\mathrm{safe}} \|\mathbf{C}(\bar{x}_{\mathrm{nom}} - \bar{p}_{\mathrm{obs}})\|_2\Big) \geq 1 - \epsilon_{\mathrm{col}}, \quad (63)$$

in robot state distribution x is a conservative approximation of the nonlinear collision chance constraint in (62) at any time $t \in [t_0, t_f]$, where $\bar{x}_{\mathrm{nom}}$ is a realization of the nominal state distribution x_{nom} of the robot that satisfies (62), $\bar{p}_{\mathrm{obs}}$ is the state of the obstacle, and $r_{\mathrm{safe}} = r_{\mathrm{rob}} + r_{\mathrm{obs}}$.

Proof: Consider the set $\mathcal{X}_{\mathrm{free}}$, defined as $\mathcal{X}_{\mathrm{free}} = \{x : \|\mathbf{C}(x - \bar{p}_{\mathrm{obs}})\|_2 \geq r_{\mathrm{safe}}\}$. Given a nominal trajectory x_{nom}, the set $\mathcal{X}_s$ defined as $\mathcal{X}_s = \{x : (\bar{x}_{\mathrm{nom}} - \bar{p}_{\mathrm{obs}})^\top \mathbf{C}^\top \mathbf{C}(x - \bar{p}_{\mathrm{obs}}) \geq r_{\mathrm{safe}} \|\mathbf{C}(\bar{x}_{\mathrm{nom}} - \bar{p}_{\mathrm{obs}})\|_2\}$ is such that $\mathcal{X}_s \subseteq \mathcal{X}_{\mathrm{free}}$. For a proof of $\mathcal{X}_s \subseteq \mathcal{X}_{\mathrm{free}}$ see [21]. Figure 5 shows an example of the set $\mathcal{X}_s$ and $\mathcal{X}_{\mathrm{free}}$, where the hyperplane used for linearization of the circular constraint leads to reduced feasible space. We can construct an indicator function $I_{\mathrm{free}}(x)$ such that $I_{\mathrm{free}}(x) = 1$ if $x \in \mathcal{X}_{\mathrm{free}}$ and $I_{\mathrm{free}}(x) = 0$ otherwise. Similarly, indicator $I_s(x)$ is such that $I_s(x) = 1$ if $x \in \mathcal{X}_s$ and $I_s(x) = 0$ otherwise.

$$\text{Since } \mathcal{X}_s \subseteq \mathcal{X}_{\mathrm{free}}, \ x \in \mathcal{X}_s \implies x \in \mathcal{X}_{\mathrm{free}},$$
$$\text{and } I_s(x) = 1 \implies I_{\mathrm{free}}(x) = 1. \quad (64)$$

Therefore, if $\mathbb{E}(I_s) \geq 1 - \epsilon_{\mathrm{col}}$, then $\mathbb{E}(I_{\mathrm{free}}) \geq 1 - \epsilon_{\mathrm{col}}$ with at least $1 - \epsilon_{\mathrm{col}}$ probability. Note that, $\Pr(x \in \mathcal{X}_{\mathrm{free}}) = \mathbb{E}(I_{\mathrm{free}}(x))$ and $\Pr(x \in \mathcal{X}_s) = \mathbb{E}(I_s(x))$. This implies that if the chance constraint in (63) is satisfied with probability $1 - \epsilon_{\mathrm{col}}$, then the constraint in (62) is satisfied with at least a probability of $1 - \epsilon_{\mathrm{col}}$. The distributional robustness approach can be visualized, as shown in Fig. 5, as a robust ball around the robot's state for collision checking using the convex feasible subset $\mathcal{X}_s$ of the non-convex feasible space $\mathcal{X}_{\mathrm{free}}$. ∎

Remark 6. *The constraint (63) is of the form $\Pr(a^\top x + b \leq 0) \geq 1 - \epsilon_{\mathrm{col}}$, where $a = -(\bar{x}_{\mathrm{nom}} - \bar{p}_{\mathrm{obs}})^\top \mathbf{C}^\top \mathbf{C}$, and $b = (\bar{x}_{\mathrm{nom}} - \bar{p}_{\mathrm{obs}})^\top \mathbf{C}^\top \mathbf{C} \bar{p}_{\mathrm{obs}} + r_{\mathrm{safe}} \|\mathbf{C}(\bar{x}_{\mathrm{nom}} - \bar{p}_{\mathrm{obs}})\|_2$. Using the Lemma 2, we formulate a second-order cone constraint that is used in the SCP problem for collision checking.*

B. Collision Checking with Stochastic Obstacle

We extend the linear chance constraint formulation in (63) to include uncertainty in obstacle state. Let the obstacle state distribution be $p_{\mathrm{obs}} \sim \mathcal{N}(\mu_p, \Sigma_p)$, where μ_p is the mean, Σ_p is the variance matrix, and the radius of obstacle is r_{obs}.

Assumption 3. *The obstacle state distribution p is uncorrelated to the state distribution x of the robot.*

The collision chance constraint at any time t for a state distribution x and radius r_{rob} is given as follows:

$$\Pr\left(\|\mathbf{C}(x - p_{\mathrm{obs}})\|_2 \geq r_{\mathrm{rob}} + r_{\mathrm{obs}}\right) \geq 1 - \epsilon_{\mathrm{col}}, \quad (65)$$

where both x and p_{obs} are random variables, unlike in (62).

Theorem 3. *The linear chance constraint,*

$$\Pr\Big((\bar{x}_{\mathrm{nom}} - \bar{p}_{\mathrm{obs}})^\top \mathbf{C}^\top \mathbf{C}(x - p_{\mathrm{obs}})$$
$$\geq r_{\mathrm{safe}} \|\mathbf{C}(\bar{x}_{\mathrm{nom}} - \bar{p}_{\mathrm{obs}})\|_2\Big) \geq 1 - \epsilon_{\mathrm{col}}, \quad (66)$$
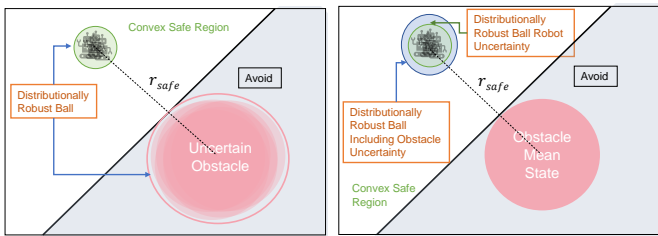
Fig. 6. An illustration of the second-order cone constraint used for collision checking with uncertainty in dynamics and the obstacle position at an instant in time is shown on the right. For a given risk of collision probability ϵ, the uncertainty in obstacle position is visualized as an additional uncertainty in the robots state.

in robot state distribution x and obstacle state distribution p_{obs} is a conservative approximation of the nonlinear collision chance constraint in (65) at any time $t \in [t_0, t_f]$, where $\bar{x}_{\text{nom}}$ is a realization of the nominal state distribution x_{nom} of the robot, $\bar{p}_{\text{obs}}$ is a realization of the obstacle state distribution p_{obs}, and $r_{\text{safe}} = r_{\text{rob}} + r_{\text{obs}}$.

Proof: Consider the sets $\mathcal{X}_{\text{free}}$ and $\mathcal{X}_s$, defined as $\mathcal{X}_{\text{free}} = \{x : \|\mathbf{C}(x - p_{\text{obs}})\|_2 \geq r_{\text{safe}}$ and $\mathcal{X}_s = \{x : (\bar{x}_{\text{nom}} - \bar{p}_{\text{obs}})^\top \mathbf{C}^\top \mathbf{C}(x - p_{\text{obs}}) \geq r_{\text{safe}}\|\mathbf{C}(\bar{x}_{\text{nom}} - \bar{p}_{\text{obs}})\|_2\}$ respectively, where $\bar{p}_{\text{obs}}$ is a sample from the obstacle state distribution p_{obs}. In the constraint $\mathcal{X}_s$, $(x - p_{\text{obs}})$ is the decision variable. Note that, for any realization of the state $\bar{x}$ and the $\bar{p}_{\text{obs}}$ we have $\mathcal{X}_s \subseteq \mathcal{X}_{\text{free}}$ (see [21] for the proof). Using the arguments in Theorem 2, the constraint (66) is a conservative approximation of the constraint (65). As shown in Fig. 6, the uncertainty in obstacle is projected as an additional uncertainty in robot's state for collision checking using the hyperplane approximation. ∎

Remark 7. *The constraint (66) is a linear chance constraint of the form* $\Pr(a^\top(x - p_{obs}) + b \leq 0) \geq 1 - \epsilon_{\text{col}}$, *where* $a = -(\bar{x}_{\text{nom}} - \bar{p}_{\text{obs}})^\top \mathbf{C}^\top \mathbf{C}$, $b = r_{\text{safe}}\|\mathbf{C}(\bar{x}_{\text{nom}} - \bar{p}_{\text{obs}})\|_2$, *and* $p_{\text{obs}} \sim \mathcal{N}(\mu_p, \Sigma_p)$. *In this case, the distributionally-robust deterministic surrogate is computed for the stacked state* $x_c = [x^\top p_{\text{obs}}^\top]^\top$, *that includes both robot and the obstacle state. The surrogate constraint is given as follows:*

$$a^\top \mu_x - a^\top \mu_p + b + \sqrt{\frac{1-\epsilon_{\text{col}}}{\epsilon_{\text{col}}}} \sqrt{a^\top \Sigma_x a + a^\top \Sigma_p a} \leq 0. \quad (67)$$

Using Lemma 6, the inequality constraint in moments is transformed to a second-order cone constraint in terms of the gPC states X *of the robot dynamics.*

Remark 8. *For correlated obstacle state* p *and robot state* x, *with the cross correlation matrix* Σ_{xp}, *the deterministic surrogate of (65) is given as follows,*

$$a^\top \mu_x - a^\top \mu_p + b + \\ \sqrt{\frac{1-\epsilon_{\text{col}}}{\epsilon_{\text{col}}}} \sqrt{a^\top \Sigma_x a + 2a^\top \Sigma_{xp} a + a^\top \Sigma_p a} \leq 0. \quad (68)$$

The derivation uses the stacked state x_c, *as shown in Remark 7.*

Remark 9. *Theorem 3 can be applied for safe multi-agent reconfiguration under uncertainty by replacing the obstacle state* p_{obs} *with the neighbouring robots state. The robots*

communicate the moments used in (68) for collision checking with the neighbouring agents.

C. Terminal Constraint

The terminal constraint is defined as an ellipsoidal set $(x - \bar{x}_f)^\top Q_{\mathcal{X}_f}(x - \bar{x}_f) \leq c_f$ around a terminal point $\bar{x}_f$, where $Q_{\mathcal{X}_f}$ is a positive definite matrix. The chance constraint formulation of the terminal set involves two steps: 1) constraining the mean of the terminal point as $\mu_f = \bar{x}_f$ and 2) formulating the quadratic chance constraint $\Pr((x - \bar{x}_f)^\top Q_{\mathcal{X}_f}(x - \bar{x}_f) \leq c_f) \geq 1 - \epsilon_f$ around the mean μ_f with risk measure ϵ_f of not reaching the terminal set. We use the conservative deterministic constraint discussed in Lemma 2, that bounds the variance of the state. The terminal constraints are summarized as follows:

$$\mu_f = \bar{x}_f, \quad \frac{1}{c_f}\text{tr}(Q_{\mathcal{X}_f}\Sigma_{x_f}) \leq \epsilon_f, \quad (69)$$

where μ_f is the mean and Σ_{x_f} is the variance of the terminal state. The conservative approximations we presented in this Section are a trade-off between the knowledge of moments available and the computational speed achieved by convex constraints. For a linear SDE with obstacles whose uncertainty is described by Gaussian distribution, a tighter equivalent deterministic surrogate constraints can be derived using the covariance propagation technique for uncertainty propagation and the inverse cumulative distribution function for Gaussian distribution.

D. Motion Planning Algorithm

For motion planning, we integrate the deterministic approximations discussed in Sections IV-A, IV-B, and IV-C with the asymptotically-optimal rapidly exploring random trees [26] (AO-RRT) algorithm. Following Algorithm 1, outlines the motion planning method using gPC-SCP for a dynamical system under uncertainty.

Algorithm 1 has three stages. In Stage 1, we formulate the linear chance constraint for collision checking and the quadratic chance constraint for the terminal constraint respectively. Using the chance constraints, we setup Problem 2 (SNOC) and project it to Problem 3 (DNOC). We formulate the gPC-SCP in Problem 4 by discretizing Problem 3. In Stage 2, we use AO-RRT to compute an initial feasible trajectory $\{\mathcal{X}_{\text{sol}}^0, \mathcal{U}_{\text{sol}}^0\}$ for the nominal dynamics $\dot{x} = f(x, \bar{u})$. In Stage 3, the feasible trajectory is then used to initialize the SCP iterations in gPC-SCP, that optimizes for the uncertainty in dynamics. The output of stage 3 is a safe and optimal state trajectory in gPC space. Using the gPC polynomials in (28), the gPC space trajectory is projected back to the state space distribution to output $\{\mathcal{X}_{\text{sol}}, \mathcal{U}_{\text{sol}}\}$ in line 12 of Algorithm 1. Note that RRT in AO-RRT can be replaced with sparse tree [63] algorithm for improved speed and with RRT* [64] for optimality. We discuss the application of Algorithm 1 in Section VI.

Algorithm 1: Distributionally-Robust Motion Planning.

Input: Map, obstacle location, x_0, $\mathcal{X}_f$, Δt, ℓ,
Input: Uncertainty model of $g(x, \bar{u})$ in SDE (7).
Output: Optimal and safe state distribution
$\qquad \mathcal{X}_{\text{sol}} = \{x_0, x_1, ..., x_T\}$ and control input
$\qquad \mathcal{U}_{\text{sol}} = \{\bar{u}_0, \bar{u}_1, ..., \bar{u}_{T-1}\}$.
$\quad \triangleright$*Stage 1: gPC Projection.*
1 Problem 3 ← **gPC Projection**
2 $\quad$ Formulate the collision constraint
$\qquad$ using Theorems 2 and 3,
3 $\quad$ Formulate the terminal set $\mathcal{X}_f$ using (69),
4 $\quad$ Project the SDE using (30),
5 $\quad$ Project the collision constraint using Lemma 6,
6 $\quad$ Project the terminal set using Lemma 7,
7 $\quad$ Setup and project cost function using (38),
8 $\quad$ **return:** Problem 3 in gPC space.

9 Problem 4 ← **Linearize** (**Discretize**
$\quad$ (Problem 3))
10 Save Problem 4.
$\quad \triangleright$*Stage 2: Compute a nominal*
$\quad$ *trajectory using AO-RRT.*
11 $\{\mathcal{X}_{\text{sol}}^0, \mathcal{U}_{\text{sol}}^0, T\}$ ← **AO-RRT** $(x_0, \mathcal{X}_f, \Delta t, \dot{x} = f(x, \bar{u}))$
$\quad$ /* For detailed implementation of
$\quad$ AO-RRT see [26]. */
$\quad \triangleright$*Stage 3: gPC-SCP.*
12 $\{\mathcal{X}_{\text{sol}}, \mathcal{U}_{\text{sol}}\}$ ←**SCP** (Problem 4,$\{\mathcal{X}_{\text{sol}}^0, \mathcal{U}_{\text{sol}}^0, T\}$)
$\quad$ /* The sequential convex programming
$\quad$ (SCP) approach is described
$\quad$ in Section III-D. */

V. TRACKING CONTROL USING STOCHASTIC MODEL PREDICTIVE CONTROL

We derive a stochastic model predictive control (SMPC) algorithm using gPC-SCP for the nonlinear control affine system defined as follows:

$$dx = f(x)dt + B(x)\bar{u}dt + g(x, \bar{u})dw, \qquad (70)$$

to track a desired state and control trajectory $(\bar{x}_{\text{des}}(t), \bar{u}_{\text{des}}(t))$, that is at least $\mathcal{C}^2$ continuous and defined $\forall t \in [t_0, t_f]$. In the SMPC approach, we solve Problem 2 for a fixed time horizon $[t_0, t_h]$, where $t_0 \leq t_{\mathcal{S}} < t_h < t_f$, and apply the control input at the time t_0. The control input $\bar{u}$ is state dependent, i.e., $\bar{u} = \bar{u}(x)$, as the SMPC problem is solved at each sample time $t_{\mathcal{S}}$ with an estimate of the current state $\bar{x}(t_{\mathcal{S}})$ as an input. The SMPC approach discussed below will ensure safety of the system in real-time at the control stage.

A. Continuous-time SMPC for Reference Tracking

We first present the continuous-time SMPC problem and then discuss the conditions for convergence and stability in terms of probability. The finite-horizon SMPC problem for tracking a desired trajectory $(\bar{x}_{\text{des}}, \bar{u}_{\text{des}})$ in the error state $\delta x = x - \bar{x}_{\text{des}}$ and the control $\delta \bar{u} = \bar{u} - \bar{u}_{\text{des}}$ is given by the following Problem 5. The desired trajectory $(\bar{x}_{\text{des}}(t), \bar{u}_{\text{des}}(t))$

is computed for the nominal dynamics $dx = f(x)dt + B(x)\bar{u}dt$ by using a deterministic motion planning algorithm. Note that the desired trajectory is still a feasible trajectory for the SDE (70). Hence, the desired trajectory could be unsafe in the presence of a white noise in the dynamics. We assume that the full state information is available to the controller.

Problem 5. *Continuous-Time SMPC.*

$$J_{\mathcal{S}_0}^* = \min_{\delta x, \delta \bar{u}} \mathbb{E}\left[\int_{t_0}^{t_h} J_{\mathcal{S}}(\delta x(t), \delta \bar{u})dt + J_{\mathcal{S}_f}(\delta x(t_h))\right] \quad (71)$$

$$\text{s.t. } d\delta x = \Delta f dt + \Delta B dt + g(x, \bar{u})dw \qquad (72)$$

$$x \in \mathcal{X}_{\mathcal{S}_{\text{safe}}}, \forall t \in [t_0, t_h], \ x(t_h) \in \mathcal{X}_{\mathcal{S}_f} \qquad (73)$$

$$\mathbb{E}(x(t_0)) = \mu_{x_0}, \ \bar{u} \in \mathcal{U} \qquad (74)$$

where $\Delta f(x, \bar{x}_{\text{des}}) = f(x) - f(\bar{x}_{\text{des}})$, $\Delta B(x, \bar{u}, \bar{x}_{\text{des}}, \bar{u}_{\text{des}}) = B(x)\bar{u} - B(\bar{x}_{\text{des}})\bar{u}_{\text{des}}$, $x(t_h)$ is the terminal state, and $\bar{x}_0$ is an estimate of the system's state at t_0. We solve Problem 5 at each time $t_{\mathcal{S}} = t_0 + k\Delta t$ for the horizon $[t_{\mathcal{S}}, t_h + k\Delta t]$, where Δt is the sampling time interval and $k \in \mathbb{Z}^+$ is the time step respectively. The cost functional $J_{\mathcal{S}}$ in (71) is defined as follows:

$$J_{\mathcal{S}}(\delta x, \delta \bar{u}) = \delta x^\top Q \delta x + \delta \bar{u}^\top R \delta \bar{u}, \qquad (75)$$

where Q and R are positive definite matrices. The safe set $\mathcal{X}_{\mathcal{S}_{\text{safe}}}$ in (73) is defined using joint linear chance constraints:

$$\mathcal{X}_{\mathcal{S}_{\text{safe}}} = \{x | \Pr(\wedge_i a_i^\top x + b_i \leq 0) \geq 1 - \epsilon_i \ \forall t \in [t_0, t_f]\}. \quad (76)$$

The terminal constraint set $\mathcal{X}_{\mathcal{S}_f}$ in (73) is defined using a quadratic chance constraint as follows:

$$\mathcal{X}_{\mathcal{S}_f} = \{x \mid \Pr(\delta x_{t_h}^\top Q_{\mathcal{X}_f} \delta x_{t_h} \leq c_f) \geq 1 - \epsilon_f\}, \qquad (77)$$

where $\delta x_{t_h} = x(t_h) - \bar{x}_{\text{des}}(t_h)$ and $Q_{\mathcal{X}_f}$ is a positive definite matrix. The matrix $Q_{\mathcal{X}_f}$ and the bound c_f in the quadratic constraint (77) are designed to be a sub-level set of the positive control invariant and reachable set of the dynamics (72) in Problem 5. Using a reachable set as the terminal constraint guarantees the feasibility of Problem 5 at each sample time $t_{\mathcal{S}} \in [t_0, t_f]$. The terminal cost $J_{\mathcal{S}_f}$ enables tracking of the desired trajectory by ensuring the stability of SMPC (Problem 5), as discussed in Section V-B.

B. Convergence and Stability

The control problem is to track the desired trajectory $(\bar{x}_{\text{des}}, \bar{u}_{\text{des}})$, i.e., $\lim_{t \to \infty} \mathbb{E}(\|x - \bar{x}_{\text{des}}\|_2^2) \leq c_t$, while ensuring that $x \in \mathcal{X}_{\mathcal{S}_{\text{safe}}}$, where c_t is an upper bound on the tracking error. The finite-horizon stochastic model predictive closed-loop system might be unstable. To guarantee tracking of the desired trajectory and the stability of the system (72), the terminal cost function $J_{\mathcal{S}_f}$ should represent the truncated cost of the infinite-horizon optimal control problem. An approach to achieve stability (see [65], [66]) in deterministic nonlinear model predictive control is to have a control Lyapunov function as the terminal cost. We use a Stochastic Control Lyapunov Function (SCLF) [25], [67], as the terminal cost for guaranteeing the stability of the SDE system (72). This is an extension of the approach discussed in [41] and [42] for discrete-time Markov decision process. We make the following

assumptions to ensure feasibility and constraint satisfaction of the Problem 5 for studying the convergence and stability of the closed-loop system.

Assumption 4. *The SDE in (72) is ϵ_c- controllable, as stated in Definition 1, to the terminal state $\delta x = 0$.*

Assumption 5. *The Problem 5 is initialized at the state x_0 such that $x_0 - \bar{x}_{\text{des}}(t_0) \in \mathcal{X}_{ci} \subseteq \mathcal{X}$, where $\mathcal{X}_{ci}$ is a stochastic control invariant set of the error dynamics (72) and $0 \in \mathcal{X}_{ci}$. A detailed discussion on the set-invariance of a controlled stochastic system can be found in [40], [68], [69].*

Assumption 6. *The constraint satisfaction at each sampling time, $t_\mathcal{S}$ is achieved by using the constraint tightening approach. In the constraint tightening approach, as described in [39], [70], an inner-level optimization problem is used to compute an optimal risk measure ϵ that leads to a feasible Problem 5.*

The cost functional $J_\mathcal{S}$ is a function of the quadratic polynomials in the error state δx and control $\delta \bar{u}$ and satisfies the lower bound as discussed in Remark 10.

Remark 10. *The cost functional $J_\mathcal{S}$ is convex in $[\delta x, \delta \bar{u}]$, and is lower bounded at any time $t \in [t_0, t_f]$ as follows:*

$$J_\mathcal{S} \geq \min\{\lambda_{\min}(Q), \lambda_{\min}(R)\}(\|\delta x\|_2 + \|\delta \bar{u}\|_2) \ \forall \ t, \quad (78)$$

where $\lambda_{\min}(Q)$ and $\lambda_{\min}(R)$ are the minimum eigenvalues of the positive definite matrices Q and R respectively.

In Assumption 7, we state the properties of the terminal cost $J_{\mathcal{S}_f}$ that guarantee the convergence of the cost and stability of the closed-loop system. Along with a SCLF-based terminal cost, we use a terminal constraint that is a subset of the control invariant set of the SDE (72) as discussed below.

Assumption 7. *The terminal cost $J_{\mathcal{S}_f}$ from (71) and the terminal constraint set $\mathcal{X}_{\mathcal{S}_f}$ satisfy the following conditions.*

(A1) *$\mathcal{X}_{\mathcal{S}_f} \subseteq \mathcal{X}_{ci} \subset \mathcal{X}_{\text{safe}}$, where $\mathcal{X}_{ci}$ is defined in Assumption 5 and $0 \in \mathcal{X}_{\mathcal{S}_f}$*

(A2) *The terminal cost $J_{\mathcal{S}_f}(\delta x)$ is of the following form:*

$$J_{\mathcal{S}_f} = \gamma \delta x^\top M(x,t)\delta x, \ \gamma > 0, \quad (79)$$

is a contraction metric (see [9], [47]) and is uniform bounded as follows:

$$c_{l_f}\|\delta x\|^2 \leq J_{\mathcal{S}_f}(\delta x) \leq c_{u_f}\|\delta x\|^2, \quad (80)$$

where $c_{l_f} > 0$ and $c_{u_f} > 0$, and satisfies the following inequality:

$$M(x,t)\frac{\partial F}{\partial x} + \left(\frac{\partial F}{\partial x}\right)^\top M(x,t) + \frac{d}{dt}M(x,t)$$
$$\leq -2\alpha M(x,t) \quad (81)$$

where $F = \Delta f + \Delta B$.

(A3) *We assume that $\text{tr}(g\nabla_{xx}J_{\mathcal{S}_f}g^\top) \leq c_v \ \forall (x, \bar{u}) \in \mathcal{X} \times \mathcal{U}$.*

(A4) *The terminal cost $J_{\mathcal{S}_f}$ satisfies the following inequality:*

$$\mathcal{L}J_{\mathcal{S}_f} \leq -2\gamma\alpha\delta x M(x,t)\delta x + c_v. \quad (82)$$

If we choose γ such that $2\alpha\gamma\delta x M(x,t)\delta x \geq J_\mathcal{S}$, then

$$\mathcal{L}J_{\mathcal{S}_f}(\delta x) + J_\mathcal{S}(\delta x, \delta \bar{u}) \leq c_v, \quad (83)$$

where the operator $\mathcal{L}$ is defined as $\mathcal{L}(J_{\mathcal{S}_f}) = \partial_t J_{\mathcal{S}_f} + \nabla_x J_{\mathcal{S}_f}^\top \Delta f + \nabla_x J_{\mathcal{S}_f}^\top \Delta B + \frac{1}{2}\text{tr}(\nabla_{xx}J_{\mathcal{S}_f}g(x,\bar{u})g^\top(x,\bar{u}))$, $J_{\mathcal{S}_f}(\delta x)$ is the terminal state cost, $J_\mathcal{S}(\delta x, \delta \bar{u})$ is defined in (71), and c_v is defined in the Assumption $(A3)$.

(A5) *For the SMPC feedback control $\bar{u}_\mathcal{S}$, the cost $J_\mathcal{S}$ is uniformly bounded as follows:*

$$c_l\|\delta x_\mathcal{S}\|^2 \leq J_\mathcal{S}(\delta x_\mathcal{S}, \delta \bar{u}_\mathcal{S}) \leq c_u\|\delta x_\mathcal{S}\|^2. \quad (84)$$

where $c_l > 0$ and $c_u > 0$. The coefficients c_l and c_u are a function of the eigenvalues of the positive definite matrices Q and R.

In Theorem 4, we prove that the optimal cost $J_{\mathcal{S}_k}^*$ decreases with the time step k, i.e., $J_{\mathcal{S}_{k+1}}^* \leq J_{\mathcal{S}_k}^*$, provided that Problem 5 satisfies the Assumptions 4, 5, 6, and 7. We show that a decreasing optimal cost implies that the SMPC is a stabilizing controller.

Theorem 4. *Suppose that Problem 5 satisfies Assumptions 4, 5, 6, and 7, the terminal cost $J_{\mathcal{S}_f}$ is a control contraction metric as defined in [67], and $J_{\mathcal{S}_f}$, $J_\mathcal{S}$ satisfy the inequality (83). Then,*

$$J_{\mathcal{S}_{k+1}}^* \leq J_{\mathcal{S}_k}^* + c_v, \quad (85)$$

$$J_{\mathcal{S}_k}^* = \mathbb{E}\left(\int_{t_0+k\Delta t}^{t_h+k\Delta t} J_\mathcal{S}(\delta x^*, \delta \bar{u}^*)dt\right) \quad (86)$$
$$+ \mathbb{E}(J_{\mathcal{S}_f}(\delta x^*(t_h + k\Delta t))),$$

where $J_{\mathcal{S}_k}^*$ is the optimal cost and $(\delta x^*, \delta \bar{u}^*)$ is the optimal feasible trajectory of Problem 5 for the time horizon $[t_0 + k\Delta t, t_h + k\Delta t]$, Δt and k are the sampling time interval and time step respectively. Furthermore, the control $\bar{u}_\mathcal{S}$ computed using the SMPC (Problem 5) is an exponential stabilizing control for the error dynamics in (72).

Proof: We first prove that the optimal cost of the finite-horizon SMPC (Problem 5) decreases with the time step k and then show that the decreasing optimal cost implies stability of the closed-loop system. Without loss of generality, we prove the inequality (85) for $k = 0$. This result can be extended to any k by moving the time horizon of Problem 5.

(a) Decreasing Cost: Let the optimal trajectory computed using the SMPC at the sampling time $t_0 = 0$ and $t_0 = \Delta t$ be $(\delta x_0^*, \delta \bar{u}_0^*), \forall t \in [0, t_h]$ and $(\delta x_1^*, \delta \bar{u}_1^*), \forall t \in [\Delta t, t_h + \Delta t]$, respectively. Assume that the trajectory $(\delta x_0^*, \delta \bar{u}_0^*), \forall t \in [0, t_h]$ is appended with the trajectory $(\delta x_{c_0}^*, \delta \bar{u}_{c_0}^*), \forall t \in [t_h, t_h + \Delta t]$, that is computed using an asymptotically stable controller satisfying the Assumption 7. The optimal costs for $k = 0$ and $k = 1$ are defined as $J_{\mathcal{S}_0}^*(\delta x_0^*, \delta \bar{u}_0^*)$ and $J_{\mathcal{S}_1}^*(\delta x_1^*, \delta \bar{u}_1^*)$,

respectively. Using (86), we can show the following equality:

$$
\begin{aligned}
J_{\mathcal{S}_1}(\delta x_0^*, \delta \bar{u}_0^*) = {} & J_{\mathcal{S}_0}^*(\delta x_0^*, \delta \bar{u}_0^*) - \mathbb{E}\left(\int_0^{\Delta t} J_{\mathcal{S}}(\delta x_0^*, \delta \bar{u}_0^*) dt\right) \\
& + \mathbb{E}\left(\int_{t_h}^{t_h + \Delta t} J_{\mathcal{S}}(\delta x_{c_0}^*, \delta \bar{u}_{c_0}^*) dt\right) \\
& + \mathbb{E}(J_{\mathcal{S}_f}(\delta x_{c_0}^*(t_h + \Delta t))) - \mathbb{E}(J_{\mathcal{S}_f}(\delta x_{c_0}^*(t_h))).
\end{aligned}
\tag{87}
$$

Since the cost $J_{\mathcal{S}}$ is quadratic in state and control, the term $-\mathbb{E}(\int_0^{\Delta t} J_{\mathcal{S}}(\delta x_0^*, \delta \bar{u}_0^*) dt)$ is ≤ 0. Using this inequality and by conditioning the expectation operation for a known $\delta x_{c_0}^*(t_h)$, we get the following inequality:

$$
\begin{aligned}
J_{\mathcal{S}_1}(\delta x_0^*, \delta \bar{u}_0^*) \leq {} & J_{\mathcal{S}_0}^*(\delta x_0^*, \delta \bar{u}_0^*) \\
& + \mathbb{E}\left(\int_{t_h}^{t_h + \Delta t} J_{\mathcal{S}}(\delta x_{c_0}^*, \delta \bar{u}_{c_0}^*) dt\right) \\
& + \mathbb{E}(J_{\mathcal{S}_f}(\delta x_{c_0}^*(t_h + \Delta t))) - J_{\mathcal{S}_f}(\delta x_{c_0}^*(t_h)).
\end{aligned}
\tag{88}
$$

By Dynkin's formula (see [24], [71]), we have the following equality:

$$
\begin{aligned}
& \mathbb{E}\left(J_{\mathcal{S}_f}(\delta x_{c_0}^*(t_h + \Delta t))\right) - J_{\mathcal{S}_f}(\delta x_{c_0}^*(t_h)) \\
& = \mathbb{E}\left(\int_{t_h}^{t_h + \Delta t} \mathcal{L} J_{\mathcal{S}_f}(\delta x_{c_0}^*) dt\right).
\end{aligned}
\tag{89}
$$

Using the Dynkin's equality (89) in the inequality (88), we have the following inequality.

$$
\begin{aligned}
& J_{\mathcal{S}_1}(\delta x_0^*, \delta \bar{u}_0^*) \leq J_{\mathcal{S}_0}^*(\delta x_0^*, \delta \bar{u}_0^*) \\
& + \mathbb{E}\left(\int_{t_h}^{t_h + \Delta t} \left(J_{\mathcal{S}}(\delta x_{c_0}^*, \delta \bar{u}_{c_0}^*) + \mathcal{L} J_{\mathcal{S}_f}(\delta x_{c_0}^*)\right) dt\right)
\end{aligned}
\tag{90}
$$

Using (83) in (90), we have:

$$
J_{\mathcal{S}_1}(\delta x_0^*, \delta \bar{u}_0^*) \leq J_{\mathcal{S}_0}^*(\delta x_0^*, \delta \bar{u}_0^*) + c_v
\tag{91}
$$

The trajectory $(\delta x_0^*, \delta \bar{u}_0^*)$ is a sub-optimal trajectory for the horizon $[\Delta t, t_h + \Delta t]$. Therefore, $J_{\mathcal{S}_1}^* \leq J_{\mathcal{S}_0}^* + c_v$. Since we use linear operations in proving $J_{\mathcal{S}_1}^* \leq J_{\mathcal{S}_0}^* + c_v$, we can extend the inequality to any $k \in \mathbb{Z}^+$ by simply moving the time horizon. Thus, we have $J_{\mathcal{S}_{k+1}}^* \leq J_{\mathcal{S}_k}^* + c_v$.

(b) Stability: The control $\delta \bar{u}_{\mathcal{S}}$ computed using Problem 5 satisfies the inequality in (83) as stated in Assumption 7. Using the uniform bounds in (80) and (84), the SCLF inequality is simplified as follows for the feedback control $\bar{u}_{\mathcal{S}}$:

$$
\mathcal{L} J_{\mathcal{S}_f}(\delta x_{\mathcal{S}}) \leq -\frac{c_l}{c_{u_f}} J_{\mathcal{S}_f}(\delta x_{\mathcal{S}}) + c_v.
\tag{92}
$$

Applying the Dynkin's formula, we have the following bound.

$$
\mathbb{E}(\|\delta x_{\mathcal{S}}(t)\|^2) \leq \frac{c_{u_f}}{c_{l_f}} \mathbb{E}(\|\delta x_{\mathcal{S}}(0)\|^2) e^{-\frac{c_l}{c_{u_f}} t} + \frac{c_v c_{u_f}}{c_{l_f} c_l}
\tag{93}
$$

As $t \to \infty$, the expectation of the tracking error is bounded by $\frac{c_v c_{u_f}}{c_{l_f} c_l}$. Therefore, the closed-loop system is exponentially stable, assuming that Assumptions 4, 5, 6, and 7 are satisfied when formulating Problem 5. ∎

Note that the convergence and stability of the SMPC controller depend on the choice of the terminal cost $J_{\mathcal{S}_f}$. The cost functional $J_{\mathcal{S}_f}$ and the metric $M(x, t)$ defined in Assumption 7

are designed by using the control contraction metric discussed in [5]. In the following section, we discuss the implementation of the SMPC controller using gPC-SCP.

C. SMPC using gPC-SCP

We formulate the SMPC (Problem 5) such that recursive feasibility, constraint satisfaction, and stability is guaranteed, as discussed in Section V-B. We then solve the SMPC problem by using the gPC approach and the gPC-SCP problem. In the following Algorithm 2, we discuss the stochastic model predictive control algorithm for tracking a given desired trajectory $(\bar{x}_{\text{des}}, \bar{u}_{\text{des}})$. We generate the desired trajectory for the nominal trajectory using a deterministic motion planner.

Algorithm 2: Stochastic Model Predictive Control.

Input: Obstacle location, x_0, $\mathcal{X}_f$, Δt, T,
Input: Desired trajectory $(\bar{x}_{\text{des}}, \bar{u}_{\text{des}})$, uncertainty model of $g(x, \bar{u})$ in SDE (7).
Output: Safe control input $\mathcal{U}_{\text{sol}} = \{\bar{u}_0, \bar{u}_1, ..., \bar{u}_{T-1}\}$ to track $(\bar{x}_{\text{des}}, \bar{u}_{\text{des}})$.

1 Compute Problem 4 for Problem 5, as discussed in Algorithm 1.
2 **while** *The terminal set $\mathcal{X}_f$ not reached* **do**
3    $\mathcal{U}_{\text{sol}} \leftarrow$ **SCP** (Problem 4,$(\bar{x}_{\text{des}}, \bar{u}_{\text{des}}), T, \Delta t, x_0$)
4   Apply $\bar{u}_0$ to the system (7)
5   Update x_0 using sensor information
6   Update $(\bar{x}_{\text{des}}, \bar{u}_{\text{des}})$ based on Δt

---

In the offline stage, we compute the projected gPC-SCP problem for Problem 5. Given a desired trajectory $(\bar{x}_{\text{des}}, \bar{u}_{\text{des}})$, time interval Δt and the number of time steps T, we solve the gPC-SCP at each time step k and apply the control $\bar{u}(t_0 + k\Delta t)$ to the system. We apply the control $\bar{u}(t_0 + k\Delta t)$ to the system, until the terminal set $\mathcal{X}_f$ is reached. Note that the terminal set $\mathcal{X}_f$ is large large enough to accommodated for the tracking error bound discussed in Theorem 4. In the following Section VI, we discuss the implementation of Algorithms 1 and 2 on a three degree-of-freedom robot.

VI. SIMULATIONS AND EXPERIMENTS ON ROBOTIC SPACECRAFT SIMULATOR

We apply the gPC-SCP method in Algorithm 1 to design safe and optimal motion plans, and the SMPC Algorithm 2 to track a nominal unsafe trajectory for the three degree-of-freedom robotic spacecraft simulator dynamics [11]. For the spacecraft simulator dynamics, we conduct an empirical study via simulation to demonstrate the safety provided by Algorithms 1 and 2 in comparison to the Gaussian collision constraint [2], [3], [6], [28], [33]. We ran the simulations on an Ubuntu machine with the configuration: 7th generation Intel Core i7 process, and 16 GB RAM. We solve the SCP problem using CVXpy [72] and ECOS [73] solver. We then validate the experimental results on the spacecraft simulator hardware platform, where the motion planning and control is computed on an NVIDIA Jetson TX2 Computer.
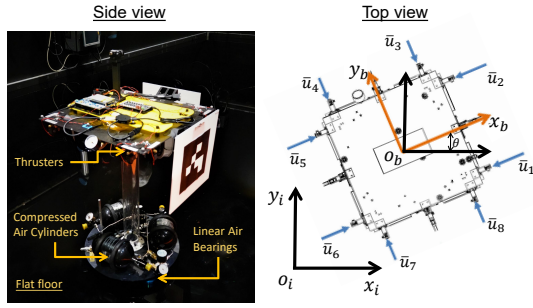
Fig. 7. The top and side view of the Caltech's robotic spacecraft dynamics simulator.

A. Robotic Spacecraft Dynamics Simulator [11]

The Caltech's M-STAR (Multi-Spacecraft Testbed for Autonomy Research) is shown in Fig. 7. The testbed floats on an ultra-precise epoxy floor using linear air bearings to achieve 3DOF friction-less motion. The M-STAR is equipped with eight thrusters for position (x, y) and yaw angle (θ) control. The dynamics of the robot is given as follows:

$$d\mathbf{x} = f(\mathbf{x}, \bar{u})dt + \sigma g(\mathbf{x}, \bar{u})dw, \quad (94)$$

where $\mathbf{x} = [x, y, \theta, \dot{x}, \dot{y}, \dot{\theta}]^\top$, $\bar{u} \in \mathbb{R}^8$, $\sigma \in \mathbb{R}$. The functions $f(\mathbf{x}, \bar{u})$ and $g(\mathbf{x}, \bar{u})$ are given below:

$$f(\mathbf{x}, \bar{u}) = \begin{bmatrix} \mathbb{I}_{3\times3} & 0 \\ 0 & 0 \end{bmatrix} \mathbf{x} + \begin{bmatrix} 0 \\ B(m, \mathrm{I}, l, \theta)\bar{u} \end{bmatrix}, \quad (95)$$

$$g(\mathbf{x}, \bar{u}) = \mathrm{blkdiag}\{0, B(m, I, l, \theta)\bar{u}\}. \quad (96)$$

The control effort $\bar{u}$ is constrained to be $0 \leq \bar{u} \leq 0.45\,\mathrm{N}$, and $B(m, \mathrm{I}, l, \theta) \in \mathbb{R}^{3\times8}$ is the control allocation matrix (see [11]), where $m = 10\,\mathrm{kg}$ and $\mathrm{I} = 1.62\,\mathrm{kg\,m\,s}^{-2}$ are the mass and the inertia matrix, and $l = 0.4\,\mathrm{m}$ is the moment arm. The uncertainty $\sigma g(\mathbf{x}, \bar{u})$ stems due to viscous friction between the robot and the flat floor, drift due to gravity gradient, and uncertainty in thruster actuation. We choose $\sigma = 0.1$, this value encompasses all the above forms of uncertainty. With this model, we study the convergence, collision checking and trajectory tracking discussed in Theorems 1, 2, 3, and 4.

B. Simulation

Consider the map shown in Fig. 8. We design a safe and optimal trajectory, $J = \|\bar{u}\|_2$, from the initial state $\mathbb{E}(x_0) = 0$ to the terminal state $\mathbb{E}(x_f) = [0.3, 2.3, 0, 0, 0, 0]^\top$, while avoiding the obstacle located at $p_{\mathrm{obs}} = [0.3, 1, 0, 0, 0, 0]^\top$ with radius $r_{\mathrm{safe}} = 0.5\,\mathrm{m}$. We formulate the collision constraint using Theorems 2 and 3 and bound the terminal variance using a slack variable to ensure feasibility. In Fig. 8, we show the mean and variance of the position of M-STAR, (x, y), computed using Algorithm 1. We compare the mean and variance computed for gPC polynomial degree $P_{\mathrm{gPC}} = \{1, 2, 3, 4\}$ and variance $\sigma = \{0.01, 0.1\}$ with $g(\mathbf{x}, \bar{u}) = [0, B\bar{u}]^\top$. The convergence of mean and variance with increasing P_{gPC}, implies convergence with respect to ℓ, validating Theorem 1. Since, there are no known methods to compute global optimal solution for Problem 1, we cannot comment on the sub-optimality of the solution. For the case with low variance
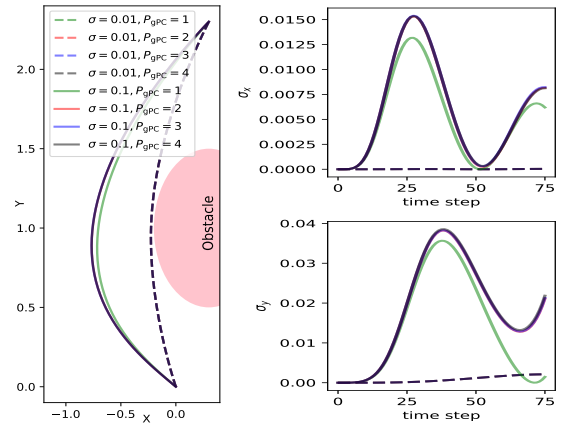

Fig. 8. The figure demonstrates convergence of the mean and the variance (σ_x, σ_y) of the states (x, y) with increasing P_{gPC} for $\sigma = \{0.01, 0.1\}$.

$\sigma = 0.01$, we observe that gPC polynomials with degree $P_{\mathrm{gPC}} = 1$ are sufficient for computing the mean and the variance accurately. While for the large variance $\sigma = 0.1$, we need gPC polynomials with degree $P_{\mathrm{gPC}} = 2$. We can use $P_{\mathrm{gPC}} = 1$ with large variance in dynamics for the following two case: 1) short-horizon planning, and 2) iterative planning with closed-loop state information updates. We use gPC polynomials with degree $P_{\mathrm{gPC}} = 2$ in the following analysis for motion planning and $P_{\mathrm{gPC}} = 1$ for SMPC-based tracking control.
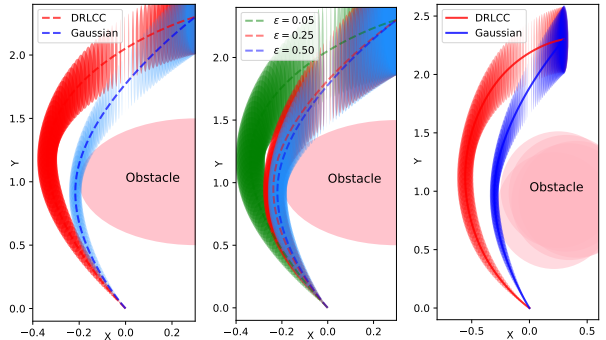

Fig. 9. Left: We compare the probabilistic safe trajectories computed using distributionally robust and Gaussian collision chance constraint. Center: We compare the trajectories for various risks ($\epsilon = 0.05, 0.25, 0.5$) of collision constraint violation. Right: We demonstrate collision checking under uncertainty in both robot dynamics and obstacle location.

1) Motion Planning: In Fig. 9, we show the mean and 2-σ confidence level of the trajectories computed using distributionally robust collision checking and Gaussian confidence-based collision checking for a risk measure $\epsilon = 0.05$. We observe that increasing the risk of collision (ϵ) in planning formulation from 0.05 to 0.5 reduces the safety in the trajectories. As shown in Fig. 9, that the trajectories generated using DRLCC are safer for obstacle with uncertainty ($\Sigma_p = 1e-4$), in comparison to a Gaussian constraint.

We validate the safety of the motion plans computed using gPC-SCP by tracking a sampled trajectory with the exponentially stable controller designed in [11] for the nominal dynamics. We sample a trajectory $\mathbf{x}$ by using the projection
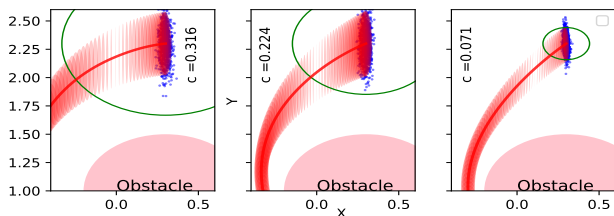
Fig. 10. We compare the trajectories generated for different sizes $c = \{0.316, 0.224, 0.071\}$ (shown as the green circle) of the terminal set. We show the terminal state of the robot (blue), when a nominal trajectory (sampled from the probabilistic trajectory) is executed using an exponentially stable controller.

equation $\mathbf{x} = \Phi^T(\xi)X$. The gPC-SCP algorithm computes the gPC coordinates X, we compute $\mathbf{x}$ by randomly sampling the multivariate normal distribution ξ. Using the motion plans shown in Fig. 9 as an input to the controller, we get the following number of collisions over 1000 trials. The number

	DRLCC	Gaussian
Deterministic Obstacle	2	41
Stochastic Obstacle ($\Sigma_p = 1e - 4$)	5	92

TABLE I
NUMBER OF COLLISIONS OVER 1000 TRAILS.

of collisions with DRLCC constraint for the risk measure $\epsilon = \{0.05, 0.25, 0.5\}$ are $\{0, 23, 181\}$, respectively. The goal reaching of the robot for various terminal variance size is shown in Fig. 10. For the terminal variance with $c = 0.071$, the robot violates the constraint 49 times over 1000 trials. Note that, although the DRLCC constraint performs better than the Gaussian constraint for nonlinear dynamical system, it reduces the feasible space of the optimization problem. For a given dynamical system and obstacle map, a trade-off analysis between distributional robustness and risk measure ϵ is required to ensure that the feasible space is non-empty.

2) SMPC-Based Trajectory Tracking: We apply the SMPC method described in Section V to track a trajectory designed using nominal dynamics $d\mathbf{x} = f(\mathbf{x}, \bar{u})dt$ with deterministic obstacles for a fixed horizon of $t_f = 25\,\text{s}$ and $\Delta t = 0.25\,\text{s}$. Since, the uncertainty in the dynamics and the obstacle location is not considered in the design of the nominal trajectory, it could be unsafe during operation. Algorithm 2 will enable safe operation, provided that Assumption 7 are satisfied. We use the Lyapunov function defined in [11] as the terminal cost $J_{\mathcal{S}_f}$, that satisfies Assumption 7 provided that the cost-to-go is defined as $Q = \mathbb{I}$ and $R = \mathbb{I}$. The terminal set is defined using the matrix $Q_{\mathcal{X}_f} = 10\mathbb{I}$. We choose $\gamma = 10$, such that the Assumption 7 is satisfied. We formulate the terminal constraint set as discussed in Section IV-C. The terminal variance is bounded using a slack variable for feasibility.

In Fig. 11, we compare the tracking performance with $\sigma = 0.1$ and uncertainty in obstacle position $\Sigma_p = \{0.01, 0.1\}$. We observe that for $\Sigma_p = 0.01$, both the proposed distributionally robust approach and Gaussian collision checking are safe for $t_h = 5\,\text{s}$. In the case with $\Sigma_p = 0.1$, the Gaussian approach has 2 failure over 5 trials for time horizon $t_h = 5\,\text{s}$. We observe that the appropriate choice of T in Problem 5 and
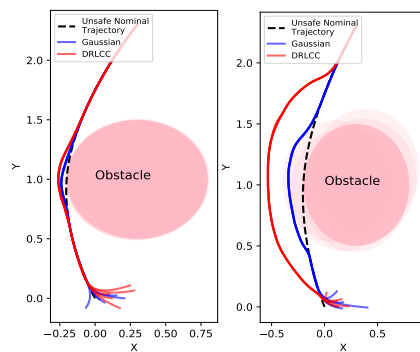

Fig. 11. We show trajectory tracking and safety under uncertainty in dynamics and obstacle location in real-time over 5 trials by using the proposed stochastic model predictive controller. We compare the distributionally robust (DRLCC) collision constraint with the Gaussian collision constraint. Left: In the case with small uncertainty ($\Sigma_p = 1e - 4$), both constraints perform safe tracking. Right: With large uncertainty ($\Sigma_p = 1e - 2$), the DRLCC provides safety in all the trials, while Gaussian collision constraint fails in 2 trials.
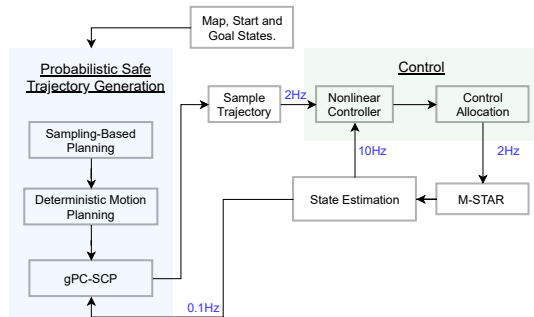

Fig. 12. The guidance, navigation and control loop used for planning a distributionally-robust safe trajectory using gPC-SCP and controlling the 3 DOF spacecraft simulators.

the cost-to-go function depend on the terminal cost $J_{\mathcal{S}_f}$, the size of the invariant set around the nominal trajectory and the uncertainty in the system and the environment. If the uncertainty is large, then the time horizon needs to be large to ensure safety. While this validates Theorem 4, further research needs to be conducted towards construction of probabilistic invariant sets for nonlinear systems to apply SMPC method for non-Hamiltonian systems.

C. Experiments

We apply Algorithm 1 for the scenario shown in Fig. 1 using the closed-loop described in Fig. 12 to design and execute safe plans for SS-1 in Fig. 1 under uncertainty in dynamics and obstacle location. This scenario is relevant to the low-earth orbit, on-orbit, servicing application discussed in [8]. Please see [11], for details on sensing module to estimate full-state, control and control allocation algorithm. We use the location of the obstacles SS-2, SS-3, SS-4, and Asteroid shown in Fig. 13, and the uncertainty in position of the obstacles $\Sigma_p = 1e - 4$ as an input to Algorithm 1. The initial state and terminal state of SS-1 are $\mathbb{E}(x_0) = [-0.9, -2.3, 0, 0, 0, 0]^\top$ and $\mathbb{E}(x_f) = [0, 2.3, 0, 0, 0, 0]^\top$, respectively.

In Fig. 13, we present the results for 10-trials of the closed-loop tracking experiment. We compute an initial anytime trajectory using AO-RRT and optimize it for nominal dynamics.
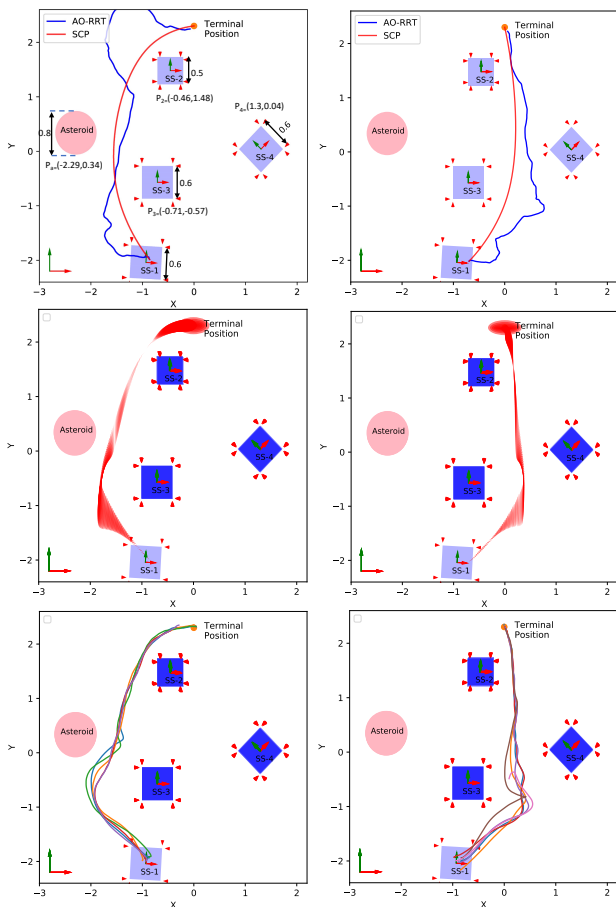
Fig. 13. We show the output of the gPC-SCP method at each stage of Algorithm 1 and 10 trials of closed-loop trajectory tracking by using an exponentially stable feedback controller designed in [11]. Top: We show the output of AO-RRT for 5000 nodes and the SCP for the nominal dynamics. Middle: We show the probabilistic safe trajectory generated using the gPC-SCP method with a risk measure of $\epsilon = 0.05$ for collision checking. Bottom: We observe one failure in the 10 trials of the closed-loop trajectory execution.

We use the optimized solution as an input for the gPC-SCP method. We observe that the method is biased towards the initial trajectory. As shown, the gPC-SCP method outputs a safe trajectory. We use the mean of the output trajectory as a reference trajectory for the controller. As shown in Fig. 13, the uncertainty in the model leads to drift in the system. The gPC-SCP method provides a safe trajectory for control by accommodating for the uncertainty in dynamics. We observe one failure out of the 10 trials of closed-loop tracking. The failure was because of a large disturbance torque on SS-1 due to a damaged floor. Out of the 10 trials, 7 closed-loop tracking trials reached the expected terminal set. This demonstrates the efficacy of the gPC-SCP method.

VII. CONCLUSION

We present a generalized polynomial chaos-based sequential convex programming method for safe and optimal motion planning and control under uncertainty in dynamics and constraints. The method uses generalized polynomial chaos projection and distributional robustness to compute a convex subset of the multi-model state-dependent chance constraints, and a high-fidelity deterministic surrogate of the stochastic dynamics and the cost functional. The surrogate deterministic optimal problem is a finite-dimensional approximation of the stochastic optimal control problem and enables the use of sequential convex programming for trajectory optimization. We study the controllability of the surrogate deterministic dynamics and propose a terminal constraint to ensure the feasibility of the surrogate optimal control problem. We prove the asymptotic convergence of the surrogate problem to the stochastic optimal control problem. The asymptotic convergence property of the deterministic surrogate allows for achieving a greater degree of safety.

We derive convex constraints for collision checking with deterministic and stochastic obstacle state models. Using these constraints, we integrate the proposed method with a sampling-based motion planning algorithm to compute safe motion plans under uncertainty in dynamics and obstacle location. We extend this method to design a stochastic model predictive control for safely tracking a nominal trajectory which is computed using a deterministic motion planning algorithm by ignoring the uncertainty. We prove the convergence and stability of the stochastic model predictive controller. We validate our approach in simulations and on the robotic spacecraft simulator hardware and demonstrate a higher success rate in ensuring the safety of motion trajectories compared to a Gaussian approximation of the chance constraints.

REFERENCES

[1] Y. K. Nakka and S. Chung, "Trajectory optimization for chance-constrained nonlinear stochastic systems," in *IEEE Conf. on Decis. and Control*, 2019, pp. 3811–3818.

[2] L. Blackmore, M. Ono, A. Bektassov, and B. C. Williams, "A probabilistic particle-control approximation of chance-constrained stochastic predictive control," *IEEE Trans. Robot.*, vol. 26, no. 3, pp. 502–517, 2010.

[3] L. Blackmore, M. Ono, and B. C. Williams, "Chance-constrained optimal path planning with obstacles," *IEEE Trans. Robot.*, vol. 27, no. 6, pp. 1080–1094, 2011.

[4] N. E. Du Toit and J. W. Burdick, "Robot motion planning in dynamic, uncertain environments," *IEEE Trans. Robot.*, vol. 28, no. 1, pp. 101–115, 2012.

[5] H. Tsukamoto and S. J. Chung, "Robust controller design for stochastic nonlinear systems via convex optimization," *IEEE Trans. Autom. Control*, pp. 1–1, 2020.

[6] H. Zhu and J. Alonso-Mora, "Chance-constrained collision avoidance for mavs in dynamic environments," *IEEE Trans. Robot. Autom. Lett.*, vol. 4, no. 2, pp. 776–783, 2019.

[7] L. P. Kaelbling and T. Lozano-Pérez, "Integrated task and motion planning in belief space," *Int.J. Robot. Res.*, vol. 32, no. 9-10, pp. 1194–1227, 2013.

[8] Y. K. Nakka, W. Hönig, C. Choi, A. Harvard, A. Rahmani, and S.-J. Chung, "Information-based guidance and control architecture for multi-spacecraft on-orbit inspection," in *AIAA GNC Conf.*, 2021, p. 1103.

[9] Y. K. Nakka, A. Liu, G. Shi, A. Anandkumar, Y. Yue, and S. J. Chung, "Chance-constrained trajectory optimization for safe exploration and learning of nonlinear systems," *IEEE Trans. Robot. Autom. Lett.*, vol. 6, no. 2, pp. 389–396, 2021.

[10] K. P. Wabersich, L. Hewing, A. Carron, and M. N. Zeilinger, "Probabilistic model predictive safety certification for learning-based control," *IEEE Trans. Autom. Control*, pp. 1–1, 2021.

[11] Y. K. Nakka, R. C. Foust, E. S. Lupu, D. B. Elliott, I. S. Crowell, S.-J. Chung, and F. Y. Hadaegh, "Six degree-of-freedom spacecraft dynamics simulator for formation control research," in *AAS/AIAA Astrodynamics Specialist Conference*, 2018.

[12] J. Ridderhof and P. Tsiotras, "Uncertainty quantication and control during mars powered descent and landing using covariance steering," in *AIAA GNC Conf.*, 2018, p. 0611.

[13] G. Shi, X. Shi, M. O'Connell, R. Yu, K. Azizzadenesheli, A. Anandkumar, Y. Yue, and S.-J. Chung, "Neural lander: Stable drone landing control using learned dynamics," in *Proc. IEEE Int. Conf. Robot. Autom.*, 2019.

[14] G. Shi, W. Hönig, X. Shi, Y. Yue, and S.-J. Chung, "Neural-swarm2: Planning and control of heterogeneous multirotor swarms using learned interactions," *IEEE Trans. Robot.*, 2021.

[15] D. Xiu and G. E. Karniadakis, "The wiener–askey polynomial chaos for stochastic differential equations," *SIAM J. Sci. Comp.*, vol. 24, no. 2, pp. 619–644, 2002.

[16] D. Xiu, "Fast numerical methods for stochastic computations: a review," *Com. in Comp. physics*, vol. 5, no. 2-4, pp. 242–272, 2009.

[17] R. G. Ghanem and P. D. Spanos, *Stochastic finite elements: a spectral approach*. Courier Corporation, 2003.

[18] A. Nemirovski and A. Shapiro, "Convex approximations of chance constrained programs," *SIAM Journal on Optimization*, vol. 17, no. 4, pp. 969–996, 2007.

[19] G. C. Calafiore and L. El Ghaoui, "On distributionally robust chance-constrained linear programs," *Journal of Optimization Theory and Applications*, vol. 130, no. 1, pp. 1–22, 2006.

[20] S. Zymler, D. Kuhn, and B. Rustem, "Distributionally robust joint chance constraints with second-order moment information," *Mathematical Programming*, vol. 137, no. 1-2, pp. 167–198, 2013.

[21] D. Morgan, S.-J. Chung, and F. Y. Hadaegh, "Model predictive control of swarms of spacecraft using sequential convex programming," *Journal of Guidance, Control, and Dynamics*, vol. 37, no. 6, pp. 1725–1740, 2014.

[22] D. Morgan, S.-J. Chung, and F. Hadaegh, "Spacecraft swarm guidance using a sequence of decentralized convex optimizations," in *AIAA/AAS Astro. Spec. Conf.*, 2012, p. 4583.

[23] D. Morgan, G. P. Subramanian, S.-J. Chung, and F. Y. Hadaegh, "Swarm assignment and trajectory optimization using variable-swarm, distributed auction assignment and sequential convex programming," *Int. J. Robot. Research*, vol. 35, no. 10, pp. 1261–1285, 2016.

[24] H. J. Kushner, "Stochastic stability and control," Brown Univ Providence RI, Tech. Rep., 1967.

[25] R. Khasminskii, *Stochastic stability of differential equations*. Springer Science & Business Media, 2011, vol. 66.

[26] K. Hauser and Y. Zhou, "Asymptotically optimal planning by feasible kinodynamic planning in a state–cost space," *IEEE Trans. Robot.*, vol. 32, no. 6, pp. 1431–1443, 2016.

[27] S. M. LaValle, *Planning Algorithms*. Cambridge University Press, 2006.

[28] N. E. Du Toit and J. W. Burdick, "Probabilistic collision checking with chance constraints," *IEEE Trans. Robot.*, vol. 27, no. 4, pp. 809–815, 2011.

[29] E. Todorov and W. Li, "A generalized iterative lqg method for locally-optimal feedback control of constrained nonlinear stochastic systems," in *Proc. of American Control Conference*, 2005, pp. 300–306.

[30] J. Van Den Berg, S. Patil, and R. Alterovitz, "Motion planning under uncertainty using iterative local optimization in belief space," *Int.J. Robot. Res.*, vol. 31, no. 11, pp. 1263–1278, 2012.

[31] J. Ridderhof, K. Okamoto, and P. Tsiotras, "Nonlinear uncertainty control with iterative covariance steering," in *IEEE 58th Conference on Decision and Control*, 2019, pp. 3484–3490.

[32] G. C. Calafiore and L. Fagiano, "Stochastic model predictive control of lpv systems via scenario optimization," *Automatica*, vol. 49, no. 6, pp. 1861–1866, 2013.

[33] L. Janson, E. Schmerling, and M. Pavone, "Monte carlo motion planning for robot trajectory optimization under uncertainty," in *Robotics Research*. Springer, 2018, pp. 343–361.

[34] G. C. Calafiore and L. Fagiano, "Robust model predictive control via scenario optimization," *IEEE Trans. Autom. Control*, vol. 58, no. 1, pp. 219–224, 2013.

[35] L. Arnold, *Stochastic differential equations*. John Wiley & Sons, 1974.

[36] M. Castillo-Lopez, P. Ludivig, S. A. Sajadi-Alamdari, J. L. Sanchez-Lopez, M. A. Olivares-Mendez, and H. Voos, "A real-time approach for chance-constrained motion planning with dynamic obstacles," *IEEE Trans. Robot. Autom. Lett.*, vol. 5, no. 2, pp. 3620–3625, 2020.

[37] L. Vandenberghe, S. Boyd, and K. Comanor, "Generalized chebyshev bounds via semidefinite programming," *SIAM review*, vol. 49, no. 1, pp. 52–64, 2007.

[38] T. Lew, R. Bonalli, and M. Pavone, "Chance-constrained sequential convex programming for robust trajectory optimization," in *Proc. Eu. Control Conf.*, 2020, pp. 1871–1878.

[39] L. Hewing and M. N. Zeilinger, "Stochastic model predictive control for linear systems using probabilistic reachable sets," in *IEEE Conf. on Dec. and Control*, 2018, pp. 5182–5188.

[40] L. Hewing, A. Carron, K. P. Wabersich, and M. N. Zeilinger, "On a correspondence between probabilistic and robust invariant sets for linear systems," in *IEEE Euro. Control Conf.*, 2018, pp. 1642–1647.

[41] D. Chatterjee and J. Lygeros, "On stability and performance of stochastic predictive control techniques," *IEEE Trans. Autom. Control*, vol. 60, no. 2, pp. 509–514, 2014.

[42] J. A. Paulson, S. Streif, and A. Mesbah, "Stability for receding-horizon stochastic model predictive control," in *IEEE American Control Conference*, 2015, pp. 937–943.

[43] A. Mesbah, S. Streif, R. Findeisen, and R. D. Braatz, "Stochastic nonlinear model predictive control with probabilistic constraints," in *IEEE American control conference*, 2014, pp. 2413–2419.

[44] V. A. Bavdekar and A. Mesbah, "Stochastic nonlinear model predictive control with joint chance constraints," *IFAC-PapersOnLine*, vol. 49, no. 18, pp. 270–275, 2016.

[45] A. M. Jasour and B. C. Williams, "Sequential chance optimization for flow-tube based control of probabilistic nonlinear systems," in *IEEE 58th Conf. on Dec. and Con.*, 2019, pp. 5392–5399.

[46] J. B. Lasserre, "Global optimization with polynomials and the problem of moments," *SIAM Journal on optimization*, vol. 11, no. 3, pp. 796–817, 2001.

[47] Q.-C. Pham, N. Tabareau, and J.-J. Slotine, "A contraction theory approach to stochastic incremental stability," *IEEE Trans. Autom. Control*, vol. 54, no. 4, pp. 816–820, 2009.

[48] A. Mesbah, "Stochastic model predictive control: An overview and perspectives for future research," *IEEE Cont. Sys. Mag.*, vol. 36, no. 6, pp. 30–44, 2016.

[49] F. S. Hover and M. S. Triantafyllou, "Application of polynomial chaos in stability and control," *Automatica*, vol. 42, no. 5, pp. 789–795, 2006.

[50] J. Fisher and R. Bhattacharya, "Stability analysis of stochastic systems using polynomial chaos," in *Proc. American Control Conference*, 2008, pp. 4250–4255.

[51] K.-K. Kim, D. E. Shen, Z. K. Nagy, and R. D. Braatz, "Wiener's polynomial chaos for the analysis and control of nonlinear dynamical systems with probabilistic uncertainties [historical perspectives]," *IEEE Control Systems Magazine*, vol. 33, no. 5, pp. 58–67, 2013.

[52] G. I. Boutselis, Y. Pan, G. De La Tore, and E. A. Theodorou, "Stochastic trajectory optimization for mechanical systems with parametric uncertainties," *arXiv preprint arXiv:1705.05506*, 2017.

[53] J. Fisher and R. Bhattacharya, "Optimal trajectory generation with probabilistic system uncertainty using polynomial chaos," *Journal of Dynamic Systems, Measurement, and Control*, vol. 133, no. 1, p. 014501, 2011.

[54] E. Buehler, "Efficient uncertainty propagation for stochastic model predictive control," Ph.D. dissertation, UC Berkeley, 2017.

[55] R. Cheng, R. M. Murray, and J. W. Burdick, "Limits of probabilistic safety guarantees when considering human uncertainty," *arXiv preprint arXiv:2103.03388*, 2021.

[56] M. Ono and B. C. Williams, "Iterative risk allocation: A new approach to robust model predictive control with a joint chance constraint," in *2008 47th IEEE Conf. on Decis. and Control*, Dec 2008, pp. 3427–3432.

[57] R. H. Cameron and W. T. Martin, "The orthogonal development of non-linear functionals in series of fourier-hermite functionals," *Annals of Math.*, pp. 385–392, 1947.

[58] T. Mühlpfordt, R. Findeisen, V. Hagenmeyer, and T. Faulwasser, "Comments on truncation errors for polynomial chaos expansions," *IEEE Cont. Sys. Let.*, vol. 2, no. 1, pp. 169–174, 2017.

[59] G. Blatman and B. Sudret, "Adaptive sparse polynomial chaos expansion based on least angle regression," *J. of Comp. Physics*, vol. 230, no. 6, pp. 2345–2367, 2011.

[60] S. Oladyshkin and W. Nowak, "Data-driven uncertainty quantification using arbitrary polynomial chaos expansion," *Reliability Engineering & System Safety*, vol. 106, pp. 179–190, 2012.

[61] Y. Xu, L. Mili, and J. Zhao, "A novel polynomial-chaos-based kalman filter," *IEEE Signal Processing Letters*, vol. 26, no. 1, pp. 9–13, 2018.

[62] E. Platen and N. Bruti-Liberati, *Numerical solution of stochastic differential equations with jumps in finance*. Springer Science & Business Media, 2010, vol. 64.

[63] Y. Li, Z. Littlefield, and K. E. Bekris, "Asymptotically optimal sampling-based kinodynamic planning," *Int.J. Robot. Res.*, vol. 35, no. 5, pp. 528–564, 2016.

[64] S. Karaman and E. Frazzoli, "Sampling-based algorithms for optimal motion planning," *Int.J. Robot. Res.*, vol. 30, no. 7, pp. 846–894, 2011.

[65] A. Jadbabaie, J. Yu, and J. Hauser, "Unconstrained receding-horizon control of nonlinear systems," *IEEE Trans. Autom. Control*, vol. 46, no. 5, pp. 776–783, 2001.

[66] D. Q. Mayne, J. B. Rawlings, C. V. Rao, and P. O. Scokaert, "Constrained model predictive control: Stability and optimality," *Automatica*, vol. 36, no. 6, pp. 789–814, 2000.

[67] H. Tsukamoto, S.-J. Chung, and J.-J. E. Slotine, "Neural stochastic contraction metrics for learning-based control and estimation," *IEEE Control Systems Letters*, vol. 5, no. 5, pp. 1825–1830, 2021.

[68] L. Billings and I. B. Schwartz, "Identifying almost invariant sets in stochastic dynamical systems," *Chaos: An Interdisciplinary Journal of Nonlinear Science*, vol. 18, no. 2, p. 023122, 2008.

[69] E. Kofman, J. A. De Doná, and M. M. Seron, "Probabilistic set invariance and ultimate boundedness," *Automatica*, vol. 48, no. 10, pp. 2670–2676, 2012.

[70] M. Lorenzen, F. Dabbene, R. Tempo, and F. Allgöwer, "Constraint-tightening and stability in stochastic model predictive control," *IEEE Trans. Autom. Control*, vol. 62, no. 7, pp. 3165–3177, 2016.

[71] B. Dynkin, *Markov processes*. Springer, 1965.

[72] S. Diamond and S. Boyd, "Cvxpy: A python-embedded modeling language for convex optimization," *J. of Mach. Learn. Res.*, vol. 17, no. 1, pp. 2909–2913, 2016.

[73] A. Domahidi, E. Chu, and S. Boyd, "Ecos: An socp solver for embedded systems," in *IEEE Euro. Control Conf.*, 2013, pp. 3071–3076.

Soon-Jo Chung (M'06–SM'12) received the B.S.degree (summa cum laude) in aerospace engineering from the Korea Advanced Institute of Science and Technology, Daejeon, South Korea, in 1998, and the S.M. degree in aeronautics and astronautics and the Sc.D. degree in estimation and control from Massachusetts Institute of Technology, Cambridge, MA, USA, in 2002 and 2007, respectively. He is currently the Bren Professor of Aerospace and Control and Dynamical Systems and a Jet Propulsion Laboratory Research Scientist in the California Institute of Technology, Pasadena,CA, USA. He was with the faculty of the University of Illinois at Urbana-Champaign during 2009–2016. His research interests include spacecraft and aerial swarms and autonomous aerospace systems, and in particular, on the theory and application of complex nonlinear dynamics, control, estimation, guidance, and navigation of autonomous space and air vehicles.

Dr. Chung was the recipient of the UIUC Engineering Deans Award for Excellence in Research, the Beckman Faculty Fellowship of the UIUC Center for Advanced Study, the U.S. Air Force Office of Scientific Research Young Investigator Award, the National Science Foundation Faculty Early Career Development Award, an Honorable Mention for the 2020 IEEE R-AL Best Paper Award, and three Best Conference Paper Awards from the IEEE and the American Institute of Aeronautics and Astronautics. He is an Associate Editor of IEEE TRANSACTIONS ON AUTOMATIC CONTROL and Journal of Guidance, Control, and Dynamics. He was an Associate Editor of IEEE TRANSACTIONS ON ROBOTICS.

Yashwanth Kumar Nakka received the B. Tech. in aerospace engineering from the Indian Institute of Space Science and Technology, India, in 2011, and the M. Sc. degree in aerospace engineering from University of Illinois Urbana-Champaign, IL, USA, in 2016 and the M. Sc. degree in space engineering from California Institute of Technology, CA, USA, in 2017. He is currently a PhD. candidate in the department of aerospace, California Institute of Technology. He was an engineer for the GSAT-15 and 16 missions at the Indian Space Research Organization during 2011-2014. His research interests include spacecraft autonomy, motion planning and control under uncertainty, and nonlinear dynamics and control.

He received the best student paper award at the 2021 American Institute of Aeronautics and Astronautics Guidance, Navigation, and Controls conference and the best paper award at the 11th International Workshop on Satellite Constellations and Formation Flying.